



First record of late Campanian paleoceanographic and paleoclimatic changes, Arabian Platform, Mazidag-Mardin area, SE Turkey

İsmail Ömer YILMAZ^{1,2}

Izzet HOŞGÖR³

Sevinç ÖZKAN-ALTINER^{1,4}

Michael WAGREICH⁵

Jiří KVAČEK⁶

Abstract: The sedimentology, geochemistry and paleontology of the pelagic upper Campanian Maastrichtian Bozova Formation in the "Mazidag" (Mazıdağı) - Mardin area, SE Turkey, reveal paleoceanographic and paleoecological changes for the first time. A 119.25 m-thick composite stratigraphic section is characterized by alternating marls, clayey limestones, shales, and black shales; no coarse siliclastic admixture or turbidite intercalations were recorded in the section. Biostratigraphic data indicate the presence of the *Radotruncana calcarata* Zone, and the UC15de/UC16 nannofossil zones. Stable isotope and elemental geochemical analyses have been carried out in the studied section. The isotope curves display similar patterns compared to reference curves from European and Chinese basins in the same interval. The prominent negative carbon isotope excursion determined in the upper interval can be correlated with the Late Campanian Event. Proxy elements display generally two relative rising - trends in productivity from the lower part and the middle part of the succession. The lower part of the section records relatively more dysoxic/anoxic conditions and coincides with common black shale beds. The presence of both diverse planktonic foraminifera and calcareous nannofossils in the studied interval indicates a fully marine, warm-water, low-latitude Tethysian oceanic environment. In addition, the plant fossils derived from the nearby land mass indicate that a tropical humid climate was similar to that in northeast Australia. Therefore, warm water, tropical humid atmospheric conditions developed in the studied area causing the rise in productivity, precipitation and transportation of plant debris into offshore environments.

Key-words:

- upper Campanian;
- paleoceanographic event;
- paleoclimate;
- plant fossil;
- Arabian Platform;
- SE Turkey

Citation: YILMAZ I.Ö., HOŞGÖR I., ÖZKAN-ALTINER S., WAGREICH M. & KVAČEK J. (2021).- First record of late Campanian paleoceanographic and paleoclimatic changes, Arabian Platform, Mazidag-Mardin area, SE Turkey.- *Carnets Geol.*, Madrid, vol. 21, no. 6, p. 137-162.

¹ Department of Geological Engineering, Middle East Technical University, 06800 Ankara (Turkey)

² ioyilmaz@metu.edu.tr

³ Çalık Petrol, Oil and Gas Directorate, 06520 Söğütözü, Ankara (Turkey)

izzet.hosgor@calikpetrol.com

⁴ altiner@metu.edu.tr

⁵ University of Vienna, Center for Earth Sciences, Department of Geodynamics and Sedimentology (Austria)

michael.wagreich@univie.ac.at

⁶ Department of Palaeontology, National Museum Prague, Václavské náměstí 68, 115 79 Praha 1 (Czech Republic)

jiri_kvacek@nm.cz





Résumé : Premier enregistrement des modifications paléo-océanographiques et paléo-climatologiques au Campanien supérieur, Plate-Forme Arabe, secteur de Mazidag-Mardin area, Turquie du sud-est.

La sédimentologie, la géochimie et la paléontologie des dépôts pélagiques d'âge Campanien supérieur à Maastrichtien de la Formation de Bozova illustrent pour la première fois les changements paléo-océanographiques dans le secteur de Mazıdağı-Mardin, Turquie du sud-est. La coupe stratigraphique composite, épaisse de 119,25 m, est constituée d'alternances de marnes, calcaires marneux, argiles et argiles noires ("black shales") ; aucun mélange grossier silicoclastique ou intercalation de turbidite n'a été observé dans cette coupe. Les données biostratigraphiques indiquent la présence de la Zone à *Radotruncana calcarata* et des zones de nannofossiles UC15de/UC16. Les analyses géochimiques d'isotopes stables et d'éléments-traces ont été effectuées sur la coupe étudiée. Les courbes isotopiques résultantes montrent des variations similaires aux courbes de référence des bassins européens et chinois pour la même période. L'excursion principale négative en isotopes du carbone reconnue dans l'intervalle supérieur peut être corrélée avec l'Événement du Campanien supérieur. Les éléments-traces montrent de manière générale deux tendances haussières relatives de la productivité dans la partie inférieure et la partie moyenne de la succession lithologique. La partie inférieure de la coupe montre des conditions relativement plus dysoxygènes/anoxiques et coïncide avec les niveaux habituels de "black shales".

La présence conjointe de foraminifères planctoniques et de nannofossiles calcaires diversifiés dans l'intervalle étudié indique un environnement marin océanique téthysien de basse latitude et d'eaux chaudes. De plus, les fossiles de plantes provenant de la masse continentale voisine indiquent un climat tropical humide similaire à celui de l'actuelle Australie nord-orientale. Par conséquent, des conditions atmosphériques tropicales humides et d'eaux chaudes se sont développées dans la zone d'étude provoquant une hausse de la productivité, des précipitations et le transport de débris végétaux jusqu'aux environnements marins du grand large.

Mots-clefs :

- Campanien supérieur ;
- événement paléo-océanographique ;
- paléo-climat ;
- fossiles de plante ;
- Plate-Forme Arabe ;
- Turquie du sud-est

1. Introduction

The Late Cretaceous, especially late Campanian paleoceanographic/paleoclimatic changes have been studied in various parts of the world by different methods to characterize the key transitional time from the mid-Cretaceous hot-house to a cooler greenhouse climate state (HU *et al.*, 2012; HAY & FLOEGEL, 2012). Most of the studies include chemostratigraphic records such as those from the European basins (JARVIS *et al.*, 2002, 2006). Lower and middle Campanian black shales and positive carbon isotope excursions in pelagic sequences are evidence of minor oceanic anoxic events (OAEs) in pelagic sequences from different parts of the world (JARVIS *et al.*, 2002, 2006; LI *et al.*, 2006; WAGREICH, 2009; LOCKLAIR *et al.*, 2011). These events correspond to the end of the OAE3 interval, which took place mainly during the late Coniacian-Santonian interval (BECKMANN *et al.*, 2005; WAGREICH, 2009; WAGREICH *et al.*, 2012).

JARVIS *et al.* (2002) correlated Campanian oceanographic changes based on carbon isotope events between successions in Tunisia, France and UK, and identified three events: (1) the positive Santonian-Campanian boundary event (SCBE), (2) the positive Mid-Campanian event (MCE), and (3) the negative late Campanian event. JARVIS *et al.* (2006) later depicted a carbon-isotope reference curve for the Cenomanian-Campanian interval in the English Chalk and indicated the mid-Campanian Event and the late Campanian Event (LCE) above the SCBE. LI *et al.*

(2006) confirmed a 2 per-mil negative shift in the carbon curve in the upper Campanian pelagic limestone and marl successions from southern Tibet, China, and correlated this excursion to the LCE. In Turkey, the Campanian-Maastrichtian pelagic sequence in the Mudurnu-Goynuk basin, Sakarya Continent, has been studied by stable isotopes and elemental analyses. ACIKALIN *et al.* (2015) indicated a negative carbon-isotope excursion in the upper Campanian *G. havanensis* biozone, above the *R. calcarata* biozone, as also recognized by WAGREICH *et al.* (2012). VOIGT *et al.* (2012) discussed the global correlation of upper Campanian-Maastrichtian carbon-isotope stratigraphy and oceanographic events. They emphasized the presence of the Campanian-Maastrichtian Boundary Event (CMBE), which is a significant long-ranging negative carbon-isotope excursion with multiple peaks of about 0.3 to 1.0 per mil (VOIGT *et al.*, 2012), also recognized by WENDLER (2013).

The Campanian record of the Arabian Platform, especially the sea-level fluctuations and the related deposits and facies have been dealt with by HAQ and AL-QAHTANI (2005). They indicated a major flooding surface in the Campanian on the Arabian Platform, probably related to Late Cretaceous tectonic movements. HAQ (2014) indicated the presence of seven sequence boundaries in the Campanian. The late Campanian sea-level record according to HAQ (2014) is characterized by a sequence boundary and 100 m sea-level fall in the *R. calcarata* biozone, and CC23a/UC 16 nannofossil biozones. This sequence boundary is over-

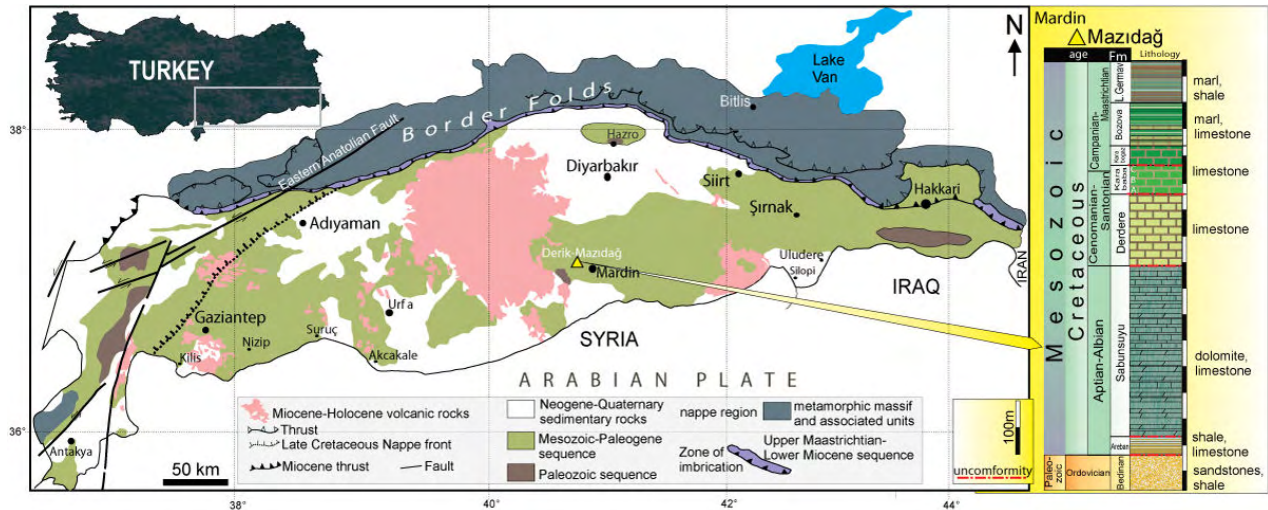


Figure 1: Simplified geological framework of Southeastern Turkey and generalised stratigraphic sequence for the Cretaceous carbonates in the Mardin-Mazıdağı region (SUNGURLU, 1974; YILMAZ *et al.*, 2018).

lain by another higher sequence boundary at the *G. aegyptiaca* biozone. According to JARVIS *et al.* (2002) the LCE seems to coincide with an interval of sea-level fall; however according to a revised sea-level change curve and sequence boundary chart of HAQ (2014), it seems to take place within the sea-level rise interval. ZAREI and GHASEMI-NEJAD (2015) indicated three Campanian sea-level falls as recorded in the Gurpi Formation on the Arabian Platform, southwest of Zagros, Iran.

Another distinct oceanographic event is the occurrence of phosphorites in Jordan (PUFAHL *et al.*, 2003) and in Israel (EDELMAN-FURSTENBERG, 2009), related to oceanic upwelling, high productivity conditions and transgressions. The records of phosphate deposition and transgressive sequences were also observed in southeastern (SE) Turkey (BEER, 1966; CATER & GILLCRIST, 1994) with the deposition of a pelagic sequence and carbonate buildups on the Arabian Platform following transgression (ERKMEN & SADEK, 1981; ÖZER, 1993).

Southeastern Turkey is situated geologically along the northern part of the Arabian Plate and is bounded to the north and east by the Iran-Zagros-Bitlis suture zone (ALA & MOSS, 1979; FONTAINE *et al.*, 1989). A thick Cretaceous sedimentary succession was deposited in this area (Fig. 1). This paper examines the Campanian succession on the Arabian Plate in southeastern Turkey using stable isotope and elemental geochemistry besides plankton biostratigraphy. The upper Campanian-Maastrichtian succession of southeastern Turkey is composed of various units (Figure 1), that reflect the intensive tectonic activity in northern parts of the region. However, carbonate successions were deposited in protected shallow marine areas (ALA & MOSS, 1979; İŞBİLİR *et al.*, 1992). This condition continued up to the end of the Paleocene and thus, except for the marginal

northern region, Şırnak, Mardin, and Gaziantep areas, no well-defined break is between the Mesozoic and Cenozoic successions (CATER & GILLCRIST, 1994).

This study provides new data for the upper Campanian-lower Maastrichtian interval in SE Turkey and discusses events and their correlations as recorded on the Arabian Platform. This study is the first application for this purpose in the Arabian Platform in SE Turkey.

2. Geological setting

During the Aptian-early Maastrichtian, southeast Anatolia lay on a shelf characterized by intrashelf basins, along the northern passive margin of the Arabian Plate (HORSTINK, 1970). The Upper Cretaceous (Campanian-Maastrichtian) sequences of the northern Arabian Platform in southeastern Anatolia are well preserved in surface and subsurface sections in SE Turkey (Fig. 1). These successions are very extensive and comprise mainly marine clastic and carbonate sedimentary rocks (HOŞGÖR & KOSTAK, 2012; MULAYIM *et al.*, 2016).

The Cretaceous sequences in the NW Mardin area are divided into seven formations (Fig. 2) composed mainly of limestones and dolomites with minor amounts of siliciclastic sequences (MULAYIM *et al.*, 2016; YILMAZ *et al.*, 2018; HOŞGÖR & YILMAZ, 2019). In the study area, basement rocks crop out close to Mazıdağı village and are characterized by Ordovician sandstone and shale (KELLOG, 1960; KURU, 1987). They are overlain by Mesozoic carbonates with an angular unconformity (SUNGURLU, 1974). The carbonate platform began to develop over the Arabian Formation (Aptian; siliciclastic sandstones and mudstones) in the studied region and the main carbonate successions, both limestones and dolomites, start

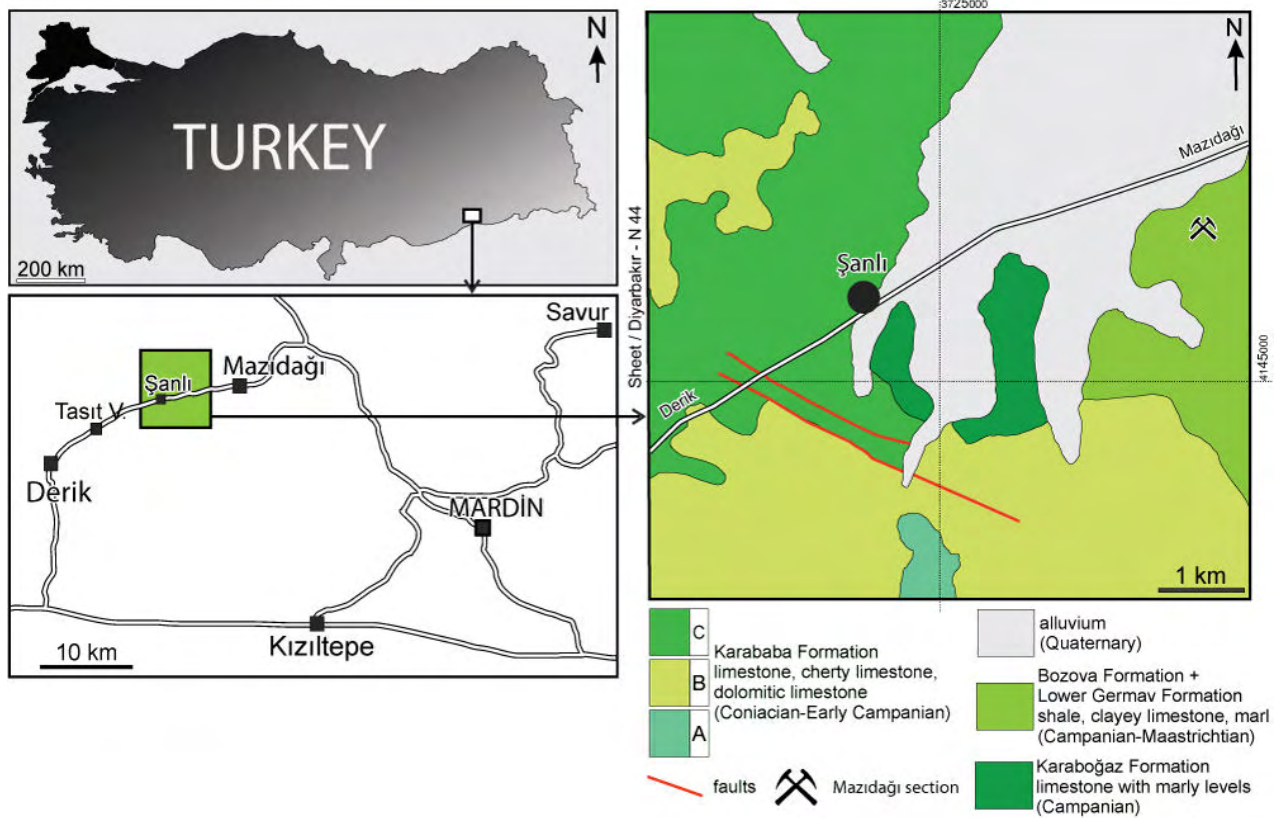


Figure 2: Geological and location map of the Mazıdağı area (after BEER, 1966; UMUT, 2011).

with the Sabunsuyu Formation (Albian). The limestones and dolomites of the Derdere Formation (Cenomanian-Turonian) overlie the Sabunsuyu Formation with an unconformity in the studied region. The Derdere is overlain unconformably by the Karababa Formation comprising limestones, cherty limestones, and dolomitic limestones of Coniacian to early Campanian age. The limestones of the Karaboğaz Formation (lower Campanian) overlie the Karababa Formation with a disconformity (Fig. 1).

The upper Campanian-Maastrichtian Bozova Formation in the Mazıdağı area is characterized by clayey limestone and marl (KÖYLÜOĞLU, 1988; ÇORUH *et al.*, 1997). The overlying Lower Germav Formation consists of calcareous mudstone-marl, and was deposited in relatively deeper, basinal conditions (CATER & GILLCRIST, 1994) as evidenced by the presence of planktonic foraminifera, plant fragments, inoceramids, and ammonites in Campanian-Maastrichtian marls, shales and limestones (YILMAZ *et al.*, 2018). The Bozova Formation on the Arabian Platform is the objective of this

study. One two-part composite stratigraphic section has been measured in detail and sampled with high frequency (Fig. 2).

3. Materials and methods

A composite stratigraphic section of the Bozova Formation is composed of two parts and was sampled in detail (Fig. 3). The sections were tied directly to each other in the field by using the bed surfaces on both sides of the road cuts. Therefore, there is no gap in between. The section is about 119.5 m thick, and 46 samples were collected. The samples were collected in regularly measured intervals in stratigraphic order (Appendix 1) but GPS measurements were not recorded per each sample. Sixteen species of planktonic foraminifera from 40 samples were identified at the Middle East Technical University, Ankara, Turkey. Loose specimens of planktonic foraminifera were picked from the rock sample residues after washing with H_2O_2 . The taxonomic criteria adopted for the identification of planktonic foraminifera are from BOLLI *et al.* (1985).

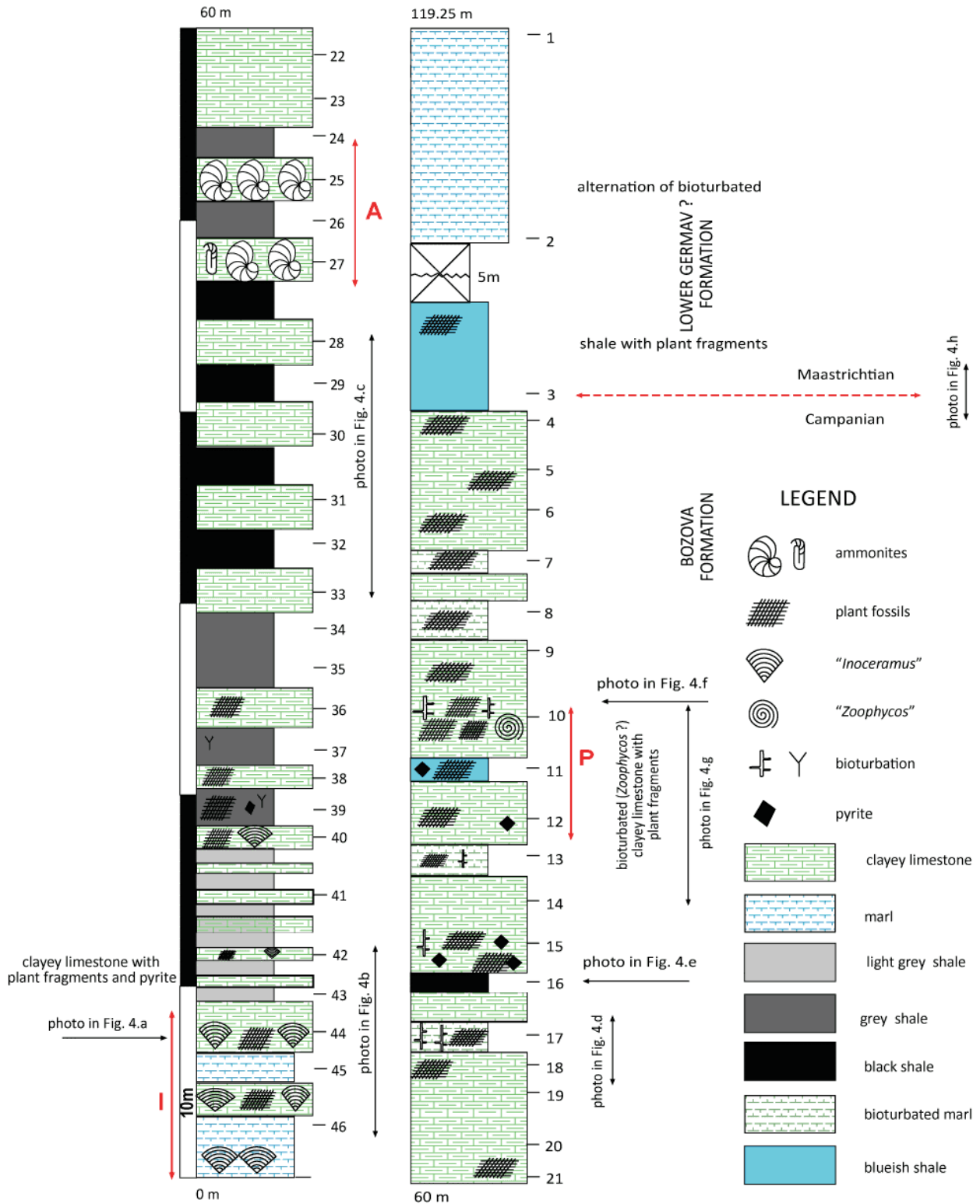


Figure 3: Mazidaği composite measured stratigraphic section of Bozova and Lower Germav Formations. Base of section is at 0 metres, sample 46, and upper part of section is 60 m to 119.25 metres, samples 1-21.

Nannofossil biostratigraphy was carried out at the University of Vienna, Department of Geodynamics and Sedimentology. Eleven smear-slide samples were prepared from a small fragment of rock dropped into distilled water for separation and determination of calcareous nannofossils

taxa. The residue was smeared onto a glass slide and fixed with Canada balsam. The samples were examined qualitatively under the polarizing light microscope (oil immersion, magnification 1000x) for nannofossil biostratigraphy.





◀ **Figure 4:** Field views of lithofacies recognized in Mažidaži section, **a)** marl with inoceramids from the lower part of the section (sample 44), **b)** lower part of the section (marls and clayey limestones with plant fragments and abundant inoceramids (I zone) (samples 46-42), **c)** middle lower part of the section (shales and marls) (samples 28-33), **d)** marl from the upper part of the section (sample 18), **e)** black shale facies recognized in the upper part of the section (sample 16), **f)** bioturbated marl with plant fossils from upper part of the section (sample 10), **g)** upper part of the section with abundant plant fossils (P zone) (marls, shales and bioturbated marls) (samples 10-14), **h)** top of the measured section (shales and marls, samples 3 and 4), the dashed red line and the letters M and C represent possible Maastrichtian and Campanian boundary.

Plant fossils were determined at the Department of Palaeontology National Museum Prague, Czech Republic. The plant fossil materials consist of twelve specimens, preserved as brown, gray, or black imprints. They are rare and slightly permineralised. The specimens were studied under a binocular microscope. Observations and photographs were made under oblique light. An Olympus CX31 polarizing microscope was used for microfacies determination, and the principles of microfacies analysis of FLÜGEL (2004) have been followed.

Stable isotope C and O analyses were carried out on 45 samples by the ISO-Analytical Company, UK using Continuous Flow-Isotope Ratio Mass Spectrometry (CF-IRMS) (the ion source of a Europa Scientific, 20-20 IRMS) with He carrier gas on-line to Gas-Bench. Finely powdered bulk rock samples were reacted with phosphoric acid to obtain CO₂. CO₂ gas liberated from samples was then analyzed by Continuous Flow-Isotope Ratio Mass Spectrometry (CF-IRMS). The reference material used for the analysis was IA-R022 (Iso-Analytical working standard calcium carbonate, $\delta^{13}\text{C}_{\text{V-PDB}} = -28.63 \text{ ‰}$ and $\delta^{18}\text{O}_{\text{V-PDB}} = -22.69 \text{ ‰}$). IA-R022 has been calibrated with the NBS-18 (carbonatite, $\delta^{13}\text{C}_{\text{V-PDB}} = -5.01 \text{ ‰}$ and $\delta^{18}\text{O}_{\text{V-PDB}} = -23.2 \text{ ‰}$) and NBS-19 (limestone, $\delta^{13}\text{C}_{\text{V-PDB}} = +1.95 \text{ ‰}$ and $\delta^{18}\text{O}_{\text{V-PDB}} = -2.2 \text{ ‰}$). The samples have been normalized according to standards and cross checked with each other for quality control. Precision of the analyses is about 0.05 and the accuracy is about 0.1 for both oxygen and carbon.

Elemental analyses of 34 samples were carried out at the Acme Analytical Laboratories Ltd., Vancouver, Canada. The total major oxides and minor elements were recovered from 0.1 g powdered limestone/marl/mudstone/shale samples (<63 mm) and analyzed by ICP-emission spectrometry and ICP-mass spectrometry following a Lithium metaborate/tetraborate fusion and dilute nitric digestion. Loss-on-ignition (LOI) was by weight-difference after ignition at 1000°C. Rare-earth and refractory elements were determined by ICP-mass spectrometry following a Lithium metaborate/tetraborate fusion and nitric acid digestion of a 0.1 g sample. In addition, a separate 0.5 g split

was digested in Aqua Regia and analyzed by ICP-mass spectrometry to report the precious and base metals. Each analysis required 5g of sample and determination limits of the elements were 0.04% for SiO₂, 0.03% for Al₂O₃, 0.04% for Fe₂O₃, 0.01% for CaO, 0.01% for MgO, 0.01% for Na₂O, 0.04% for K₂O, 0.01% for MnO, TiO₂ and P₂O₅, 0.5 ppm for Ba, 0.1ppm for Cd, Cu, Mo, Ni and Pb, 1 ppm for Zn, and 5 ppm for V.

4. Lithology and facies

Lithology and microfacies descriptions were based on field observations and petrographic analysis. Sedimentary structures observed were used to determine the depositional environments.

At the base of the lower part of the section, alternating clayey limestone is overlain by alternating marl and black shale (Figs. 3-4.b-c, .e). In this first alternation of clayey limestone and marl, the association of plant fragments, relatively abundant inoceramid shells, pyrite and relative abundance of bioturbation was remarkable (Fig. 3: samples 44-46; Fig. 4.a). Another clayey limestone - marl alternation is present at the top of the lower part of the section. At the ultimate top, clayey limestones become dominant (Fig. 4.h). Bioturbation is not intensive throughout the whole section. In this second interval of intercalated clayey limestone and marl ammonites are relatively abundant. Along the section, these relative abundance zones are indicated as I (inoceramids) and A (ammonites) to display their positions along the section (Fig. 3). Black shales are laminated, silty (Fig. 4.e) and rarely bioturbated.

Alternating clayey limestone, marl and shale characterize the bottom of the upper part of the section (Fig. 4.c, .g). Clayey limestones are thicker than the marls and increase in thickness compared to the lower part of the section. Alternating thin clayey limestone and marl are present in the topmost part of the section. Clayey limestone and marl include pyrite, fine bioturbation, relatively abundant plant fossils and fragments (Fig. 4.d, .f) marked with P in the section log (Fig. 3). Some plant fossils are also present towards the top of the section, but they stratigraphically disappear at the top (Fig. 3). The topmost part of the section displays lighter colors and does not include any plant fossils, ammonites, inoceramids, or pyrite. Transported shallow water benthic foraminifers or calcareous turbiditic facies or coarse siliciclastic intercalations have not been observed throughout the studied section.

Lithofacies analyses are parallel with the field observations and are cross-checked with petrographic examinations under the microscope (Fig. 5). The following types of facies were identified, and petrographic compositions are explained:

Shale: Shales are generally laminated and silty. Gray, light grey and blueish grey shales alternate with clayey limestones in the lower part of the section.

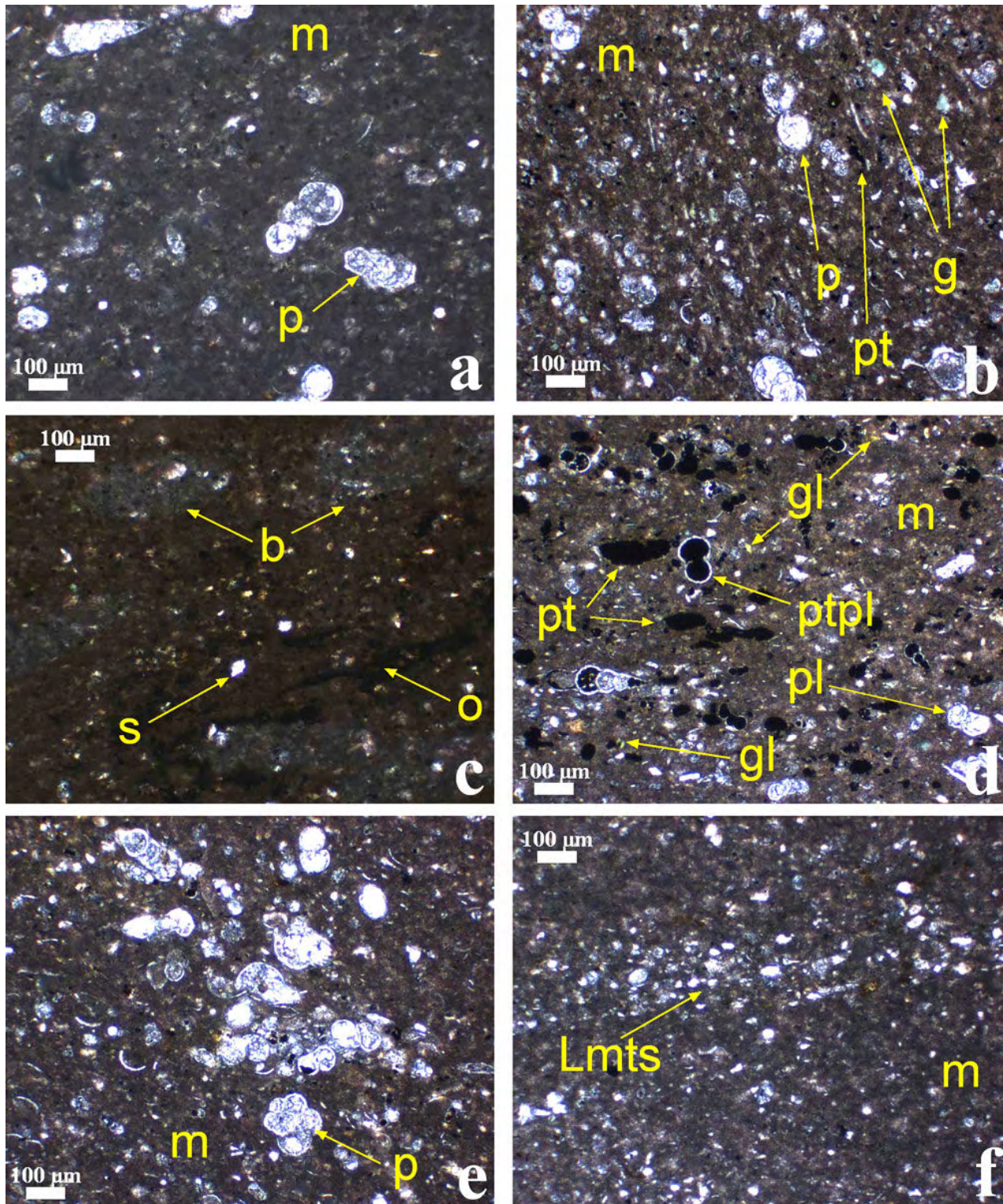


Figure 5: Photomicrographs of the microfacies recognized in Mazıdağı section. Small white bar is 100 micron scale for all, **a**) marl with planktonic foraminifera and plant fossil (p: planktonic foraminifera, m: micrite) (sample 5), **b**) bioturbated silty marl (p: planktonic foraminifera, m: micrite, pt: pyrite, g: glauconite) (sample 13), **c**) silty black shale with microbioturbation (b: microbioturbation traces, o: organic matter linings, s: silt) (sample 16), **d**) laminated clayey limestone (wackestone) with pyrite and glauconite (pt: pyrite, ptpl: planktonic foraminifera filled with pyrite, pl: planktonic foraminifera, m: micrite, gl: glauconite) (sample: 15), **e**) clayey limestone with planktonic foraminifera (packstone-wackestone) (m: micrite, p: planktonic foraminifera) (sample 18), **f**) gray silty calcareous shale (Lmts: laminated silt, m: matrix) (sample 24).

Marl: Marls are generally greyish to beige-colored, thin bedded and silty (Fig. 5.a-b). Generally, marls are more common in the bottom and

the top of the section. In some intervals, tiny bioturbation structures are in the marls. Plant fossils and fragments are also observed in the field. Ma-



trix is generally composed of micrite and clay. Pyrite and glauconite are also observed. Pyrite is disseminated in the matrix and replaced the fossil shells (Fig. 5.b). Small and large planktonic foraminifera, few peloids and very few thin bivalve fragments are present in the matrix (Fig. 5.a-b).

Black shale: Thin-bedded black shales are mainly observed in the mid part of the section. They are silty, laminated and rarely bioturbated (Fig. 5.c). Matrix of the black shale facies is generally composed of quartz silt, organic matter, clay, and micritic carbonate (Fig. 5.c). Microbioturbation structures observed petrographically are infilled by micritic calcite (Fig. 5.c).

Clayey limestone: Thin bedded light grey to beige-colored clayey wackestone to packstone alternate with marls and shales throughout the section. Ammonites and inoceramids are present and planktonic foraminifera are abundant. Micro-scale disseminated pyrite is in matrix and fills the chambers of planktonic foraminifera (Fig. 5.d-f). Fine-grained disseminated glauconite is also in clayey limestone facies together with pyrite.

5. Biostratigraphy and paleontology

Planktonic foraminifera and calcareous nannofossils are the biostratigraphic index species that define biozones. Plant fossil identifications helped to understand the paleoecological and paleogeographical conditions in the studied region.

CALCAREOUS NANNOFOSSILS

The nannofossil assemblages are characterized by common genera like *Watznaueria*, *Rectecapsa*, *Cribrosphaerella*, *Chiastozygus*, *Lithraphidites*, *Micula*, and *Microrhabdulus*. The common dominating presence of *Watznaueria barnesae*, and the lack or low amount of cold or cooler water species like *Ahmuellerella octoradiata*, *Gartnerago* spp., *Kamptnerius magnificus*, and *Arkhangelskiella cymbiformis* (e.g., LEES, 2002; THIBAUT & GARDIN, 2006, 2010; THIBAUT *et al.*, 2015) attests to a fully marine, warm-water, low-latitude Tethysian oceanic environment.

Nannofossil biostratigraphy is based on zonations by PERCH-NIELSEN (1985) and BURNETT (1998). Samples from lower part of the Mazidađi section indicate an upper Campanian age throughout, with zones CC22-CC23a (PERCH-NIELSEN, 1985) and UC15de-UC16 (BURNETT, 1998), respectively. The main nannofossil markers include *Arkhangelskiella cymbiformis*, *Broinsonia parca parca* and *Broinsonia parca constricta* (not found in all samples, Figs. 6-7), *Ceratolithoides aculeus*, *Quadrum gothicum*, *Reinhardtites levis*, *Tranolithus orionatus*, *Uniplanarius sissinghii*, and *Uniplanarius trifidus*. Biostratigraphic zone interpretation relies on the presence of both *B. parca* subspecies (last occurrence LO defines top UC16/CC23a), and *Uniplanarius trifidus* (first occurrence FO defines base of UC15d/CC22). The absence of both *Reinhardtites anthophorus* and *Eiffellithus eximius* (LOs define top of UC15/CC22) is notable

but may relate to the poor preservation of the nannofossils. A single broken specimen of *Eiffellithus eximius* in sample 19 is regarded as reworked from older sediments. In addition, *Operculodinel-la operculata* is present in most of the samples.

Samples from uppermost part of the Mazidađi section in principle show the same assemblage and marker species, with *B. parca parca*, *B. parca constricta* and *Uniplanarius trifidus*, and thus are still in zones CC22-CC23a (PERCH-NIELSEN, 1985) and UC15de-UC16 (BURNETT, 1998). The uppermost nannofossil sample of the section, sample 3, without specimens of the *B. parca* group, may indicate already the beginning of UC17/CC23b around the uppermost Campanian - lowermost Maastrichtian boundary (e.g., BURNETT, 1998; WAGREICH *et al.*, 2009). However, the planktonic foraminifera data (see below) argues against such an interpretation. Also, additional samples from isolated outcrops around Mardin yielded an upper Campanian age, mostly CC22/23a and UC15de-UC16, and no indication of younger biostratigraphic ages.

PLANKTONIC FORAMINIFERA

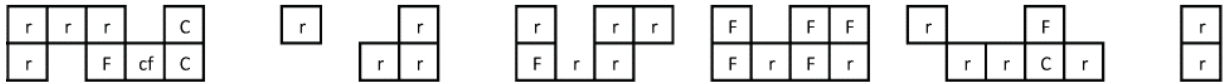
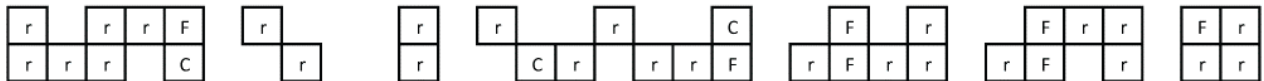
Obtaining a precise distribution of the chronologically significant taxa made several re-sampling campaigns in the field necessary to supplement the information between significant samples. As a result of this procedure, the around 120 m-thick composite section was investigated with 40 samples. The graphic section logs (Figs. 6-7) are compiled from different sections at different scales, therefore these figures present sample-based correlation not scale-based correlation.

Planktonic foraminifera are mainly scattered occurrences and are low to moderately abundant assemblages along the section. Heterohelicids, muricohedbergelids, and macroglobigerinelloids are consistently present in substantial numbers, whereas the distribution of globotruncanids is more discontinuous throughout the section (Figs. 6-7). The globotruncanids are mainly represented in the low to moderately abundant assemblages including such as *Contusotruncana fornicata*, *G. bulloides*, *G. lapparenti*, *G. linneiana*, *G. orientalis*, *G. rosetta*, *G. ventricosa*, *Globotruncanita stuartiformis*, and *Radotruncana calcarata* throughout the section (Figs. 6-7).

Although the marker species are in scattered occurrences, the conspicuous species found throughout this section and the LO and HO of *R. calcarata* define the temporal limits of the *Radotruncana calcarata* Zone (WAGREICH *et al.*, 2012). This zone is correlative with the lowermost part of the upper Campanian (GRADSTEIN *et al.*, 2012). In addition to this marker species, the presence of *Globotruncana ventricosa*, *Globotruncanella havanensis* and *Planoglobulina sp.* supports the same chronostratigraphic interval (Figs. 6-7) (GRADSTEIN *et al.*, 2012). Finally, the combination of these taxa provides a possible middle upper Campanian interval.

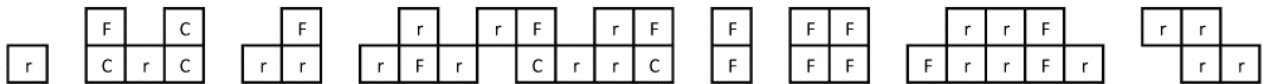


Ceratolithoides aculeus
Cretarhabdus striatus
Chiastozygus litterarius
Cribrospheraella circula
Cribrospheraella ehrenbergii
Cyclagelosphaera sp.
Cylindralithus cf. serratus
Cylindralithus sp.
Eiffelithus eximius
Eiffelithus gorkae
Eiffelithus turrisseiffeli
Gartnerago obliquum
Helicolithus ? sp.
Lithraphidites carniolensis
Lucianorhabdus cayeuxii
Manivitella pemmatolidea
Microrhabdulus decoratus
Micula quadrata
Micula stauraphora
Ocotolithus multiplus
Operculodimella operculata
Prediscosphaera cretacea
Prediscosphaera spinosa
Quadrum sp.
Quadrum gothicum
Reinhardtites levis
Retecapsa crenulata
Rhagodiscus angustus
Rhagodiscus sp.
Staurolithites crux
Tranolithus orionatus
Uniplanarius sissinghii



r=rare (1/10-50 FOV)
M=medium

F=few (1/1-10 FOV)
P=poor preservation



Paleoecological remarks: Plant fossils occurring in marine sediments are of completely allochthonous origin. However, they indirectly represent vegetation and paleoclimate occurring on nearby dry land. In the studied outcrop five specimens assigned to a new species *Araucaria rothwellii* were excavated (KVAČEK *et al.*, 2019). All species of *Araucaria* have prevailing distribution in the low mid-latitudes (KRASSILOV, 1978; KERSHAW & WAGSTAFF, 2001), in mesothermal to microthermal climates (PANTI *et al.*, 2012). The studied material indicates that *Araucaria* was a common conifer of the northern Gondwana mesophytic vegetation. *A. rothwellii* represents a broad-leaved species that probably grew in more humid environments, while araucarioid plants with imbricate leaves of *Brachyphyllum obesum* type grew in more xeric areas (compare KVAČEK *et al.*, 2018). Broad-leaved Araucariaceae are present in the Lower Cretaceous of Lebanon (POINAR & MILKI, 2001). The appearance of wood fiber inclusions, and spectroscopic studies of amber argue for Araucariaceae as sources of the Myanmar Albian-Cenomanian amber (POINAR *et al.*, 2007).

The genus *Araucaria* is an important indicator of paleoenvironments (KRASSILOV, 1978). Therefore, closer identification of the fossil is helpful for more precise paleoenvironmental interpretations. Based on comparison of macro- and micro-morphology KVAČEK *et al.* (2019) concluded that the species is most similar to *Araucaria bidwillii*. *A. bidwillii* grows in tropical rainforests in North East Australia where the annual rainfall is greater than 1000 mm (FARJON, 2010). The species is able to tolerate temperatures ranging from -4°C to 40°C (HUTH, 2002). These climatic variables support paleoecological interpretations of a Campanian paratropical humid to sub-humid climate in the area where *A. rothwellii* occurred.

6. Geochemistry

STABLE ISOTOPES

Carbon isotope values range between a minimum of 0.57 ‰ and a maximum of 1.92 ‰ and δ¹⁸O values range between -4,23 ‰ and -3.45 ‰ (Appendix 1). Stable isotope analyses reveal that carbon and oxygen isotope values are not greatly affected by diagenesis. Cross plots of the values indicate a trend line with no correlation with R² = 0.281 (Fig. 8).

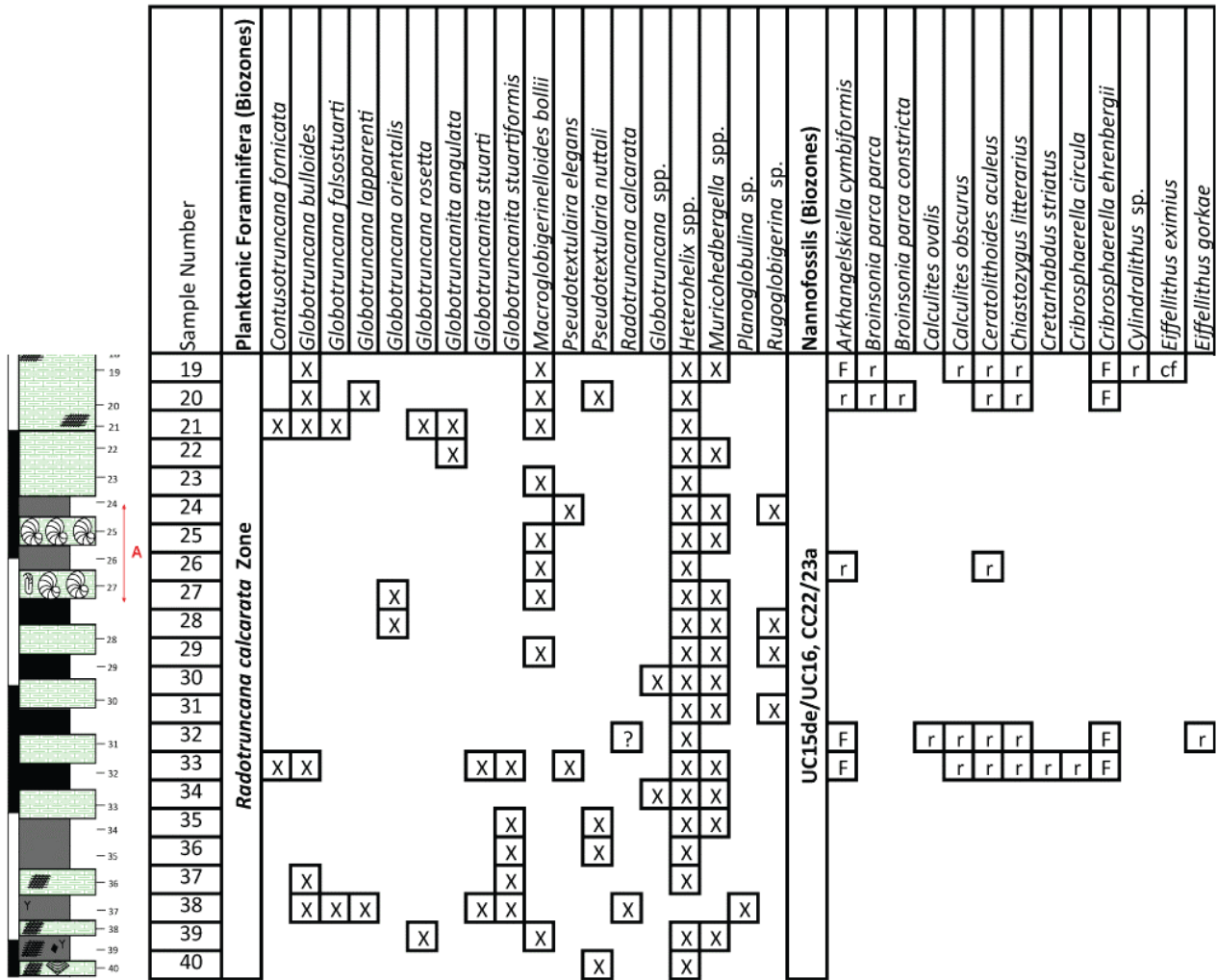


Figure 7: Distribution of nannofossil and planktonic foraminifera species in the upper part of the Bozova Formation, Mazıdağı section. (note: for symbols and legends see Fig. 3).

The carbon isotope curve displays a negative shift in the lower-mid part of the section of about 1.5 per mil change (sample 19), and then it turns into a positive shift with more than 0.5 per mil in the upper part of the section (Fig. 9). It stabilizes and then displays a negative shift at the top of the section. However, oxygen isotopes display a relatively smooth curve but fluctuate between narrow values. It has a 0.5 per mil shift in the upper part of the section (Fig. 9). This shift coincides with positive shift of the carbon isotope curve. The isotope curves are divided in to 4 intervals to better correlate the minor details in between (Fig. 9). In interval one at the bottom of the section, both curves display a similar pattern, but carbon isotope values tend to decrease towards relatively more negative values. Both curves present a 0.5 per mil negative shift at the bottom of the section. In interval two, oxygen isotope values fluctuate with 0.5 per mil and the curve displays a relatively smooth pattern. However, carbon isotope values change by more than 2 per mil; the curve shows a positive shift at the bottom of interval two and above it is a negative shift of more than 2 per mil at the top of the interval (Fig. 9).

In interval three, a positive carbon isotope shift of around 1 per mil is at the bottom and above it fluctuates around 0.5 per mil. However, oxygen isotopes present a negative shift with 0.5 per mil at the bottom and then display a positive 0.5 per mil shift at the top of the section. In interval four, both curves are relatively smooth at the bottom and mid parts of the interval. However, at the top of the interval a negative carbon shift is about 1 mil (Fig. 9). The oxygen curve varies about less than 0.5 per mil.

ELEMENTAL GEOCHEMISTRY

Generally, the oxide elements from bulk rock samples correspond to changes in isotope curves but at different magnitudes. Fluctuations in values of CaO, FeO, SiO₂, Al₂O₃, MgO, Na₂O, MnO, TiO₂, P₂O₅, Cd, Ba, Cu, Mo, Pb, Zn, and V throughout the section are herein used for interpretation such as Paleoproductivity (BURDIGE, 2006; TRIBOVILLARD *et al.*, 2006; PAYTAN, 2009; LIGUORI *et al.*, 2016), Hydrothermal and magmatic indicators (CHRISTENSEN *et al.*, 1982; OWEN & OLIVAREZ, 1988; BURDIGE, 2006; DEMINA & GALKIN, 2016) and Redox indicators (BURDIGE, 2006; TRIBOVILLARD *et al.*, 2006; MCKAY *et al.*, 2007; COLE *et al.*, 2017; GOSWAMI *et al.*, 2012) (Appendix 2).

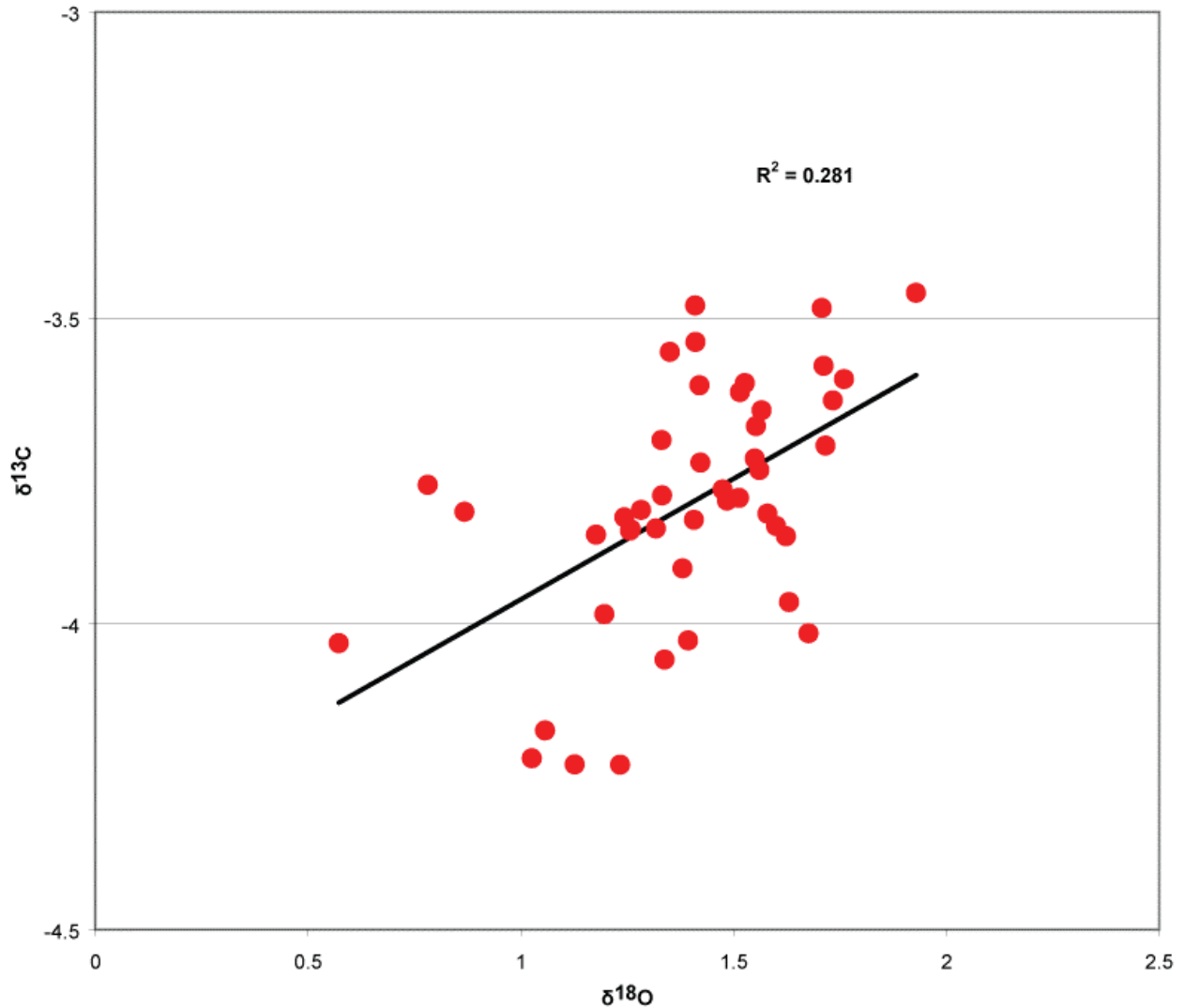


Figure 8: Cross plot of C and O stable isotope values of the Bozova Formation, Mazıdağı section. Units are per mil.

It then abruptly rises in the middle part of the section (Fig. 13) and slightly rises with fluctuations in the upper part.

Redox indicators include Mo/Al, Mn/Al, TOTS, U/Al, and Mn/Al (BURDIGE, 2006; TRIBOVILLARD *et al.*, 2006; MCKAY *et al.*, 2007; GOSWAMI *et al.*, 2012; COLE *et al.*, 2017). They decrease slightly in the lower half and increase in the upper half of the section (Fig. 14). TOTS values present a highly fluctuating pattern with higher values in the lower part of the section and decrease abruptly in the middle part (Fig. 14). In the upper half of the section, it shows high values also but the magnitude and frequency of the fluctuations are less than in the lower part. U/Al is relatively enriched in the lower part (Fig. 14). The Mo/Al curve displays high values and rising trend in the lower part and then an abrupt decrease in the middle part, whereas in the upper part of the section it has very low values and a relatively

smooth curve. The Mn/Al curve decreases into the middle part and increases into the upper part (Fig. 14).

7. Discussion

The Campanian section in the region of SE Turkey has been studied for the first time in detail and with high-resolution. Paleoclimatological and paleoceanographical implications are detected from proxy data. Previous biostratigraphic studies in the region presented a lower resolution (ÇORUH *et al.*, 1997). In the abundant plant fossil fragment zone in the studied section, the species are not diverse and physically not well preserved. Ammonite and inoceramid fossils were recorded for the first time in the study area. However, we were not able to identify the species for independent contribution to this study but will be presented in a future project.

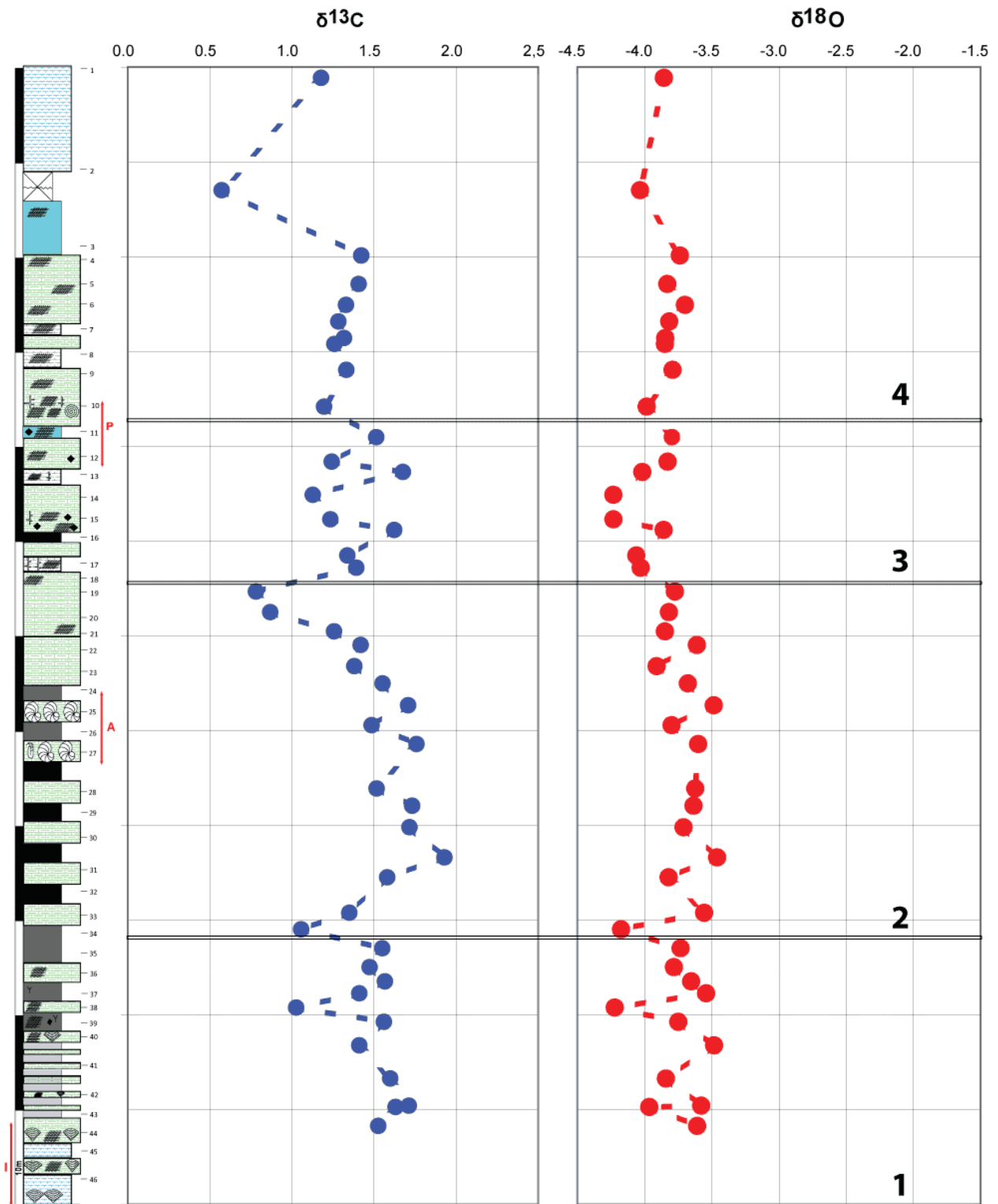


Figure 9: C and O stable isotope curves of the Bozova Formation, Mazıdağı section. Numbered rectangular boxes refer to interval divisions. Units for C and O isotope values are per mil. Lithostratigraphic column is generalized for sample and facies comparison.

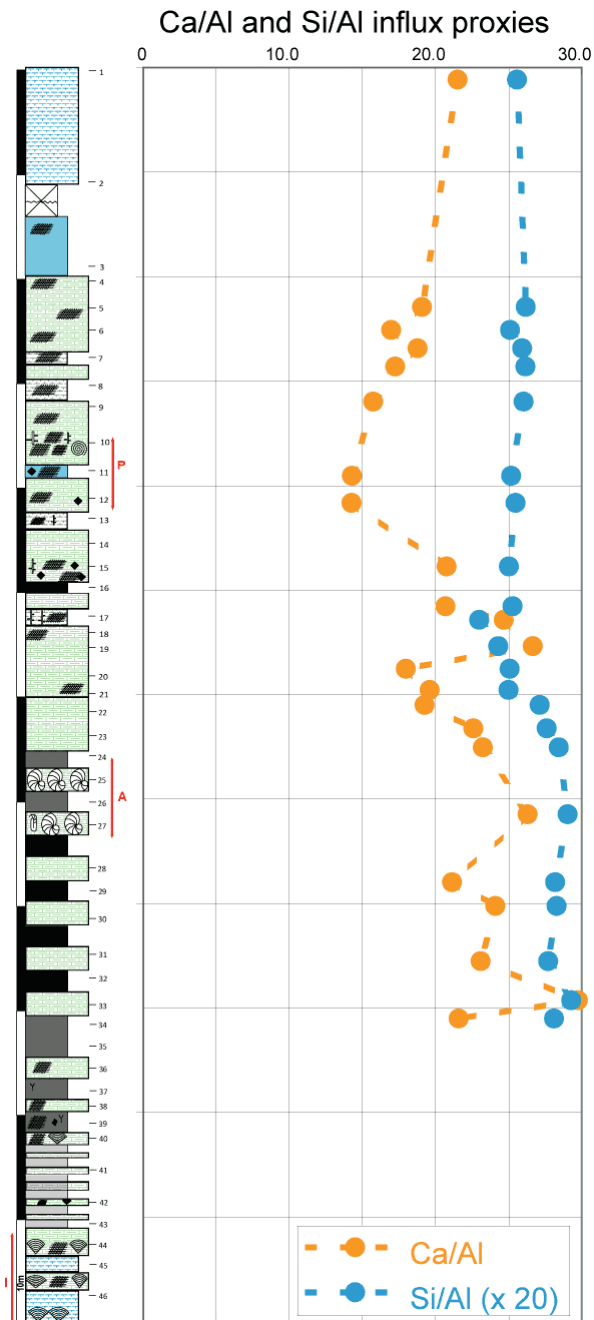


Figure 10: SiO and CaCO₃, Si/Al, Ca/Al distribution in the Bozova Formation, Mazıdağı section. Lithostratigraphic column is generalized for sample and facies comparison.

The $\delta^{13}\text{C}$ and $\delta^{18}\text{O}$ values do not appear to be strongly altered diagenetically by either the water-rock interaction or deep burial diagenesis (HOEFS, 2009; BISHOP *et al.*, 2014). Three main parts in the curve can be compared with the European (JARVIS *et al.*, 2002) and Chinese carbon isotope curves (LI *et al.*, 2006). The LCE in this section displays relatively a smaller magnitude compared to European curves. This may be related to first approach and lower resolution sampling of the LCE. Total thickness of the section is 119.25 m, which is a bit thicker than European

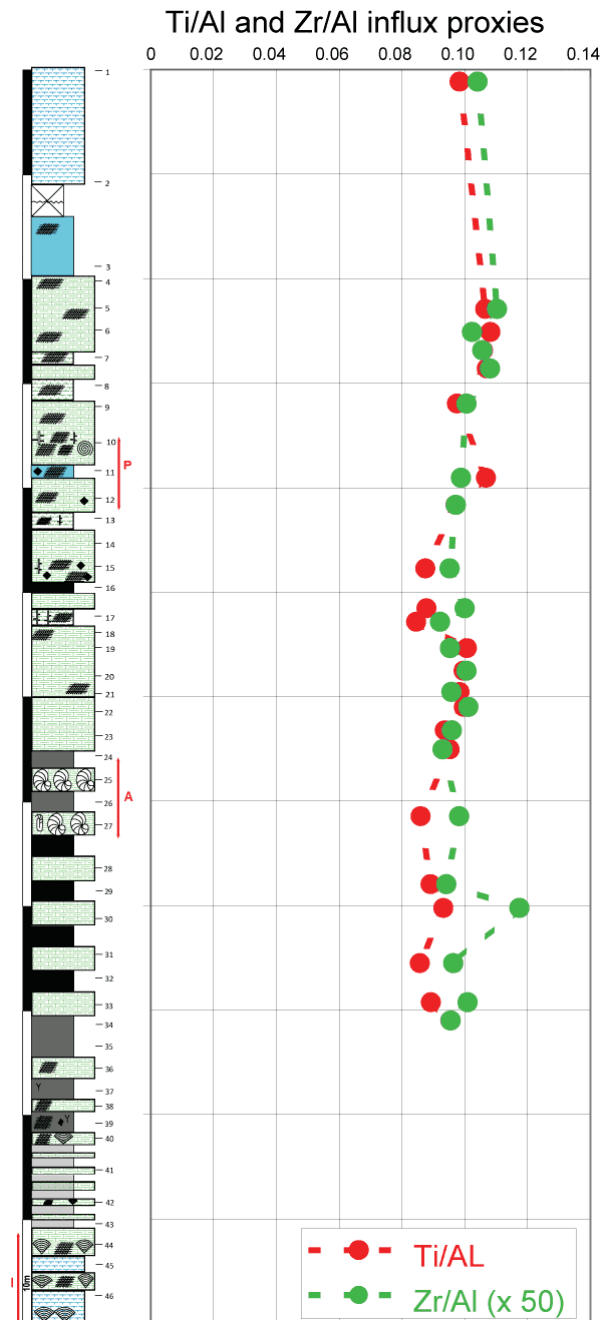


Figure 11: TiO, Zr, Ti/Al, and Zr/Al distribution in the Bozova Formation, Mazıdağı section. Lithostratigraphic column is generalized for sample and facies comparison.

sections. VOIGT *et al.* (2010) indicated a Late Campanian Event (LCE) in the isotope curve from European shelves and the Pacific Ocean in the UC15d/e biozone. However, PERDIOU *et al.* (2015) indicated the position of the LCE in UC15c in the North Sea. According to CHENOT *et al.* (2016) the LCE is observed in the UC15d/e biozone in Paris Basin, WAGREICH *et al.* (2012) reported the LCE directly above the *Radotruncana calcarata* Zone in northwestern Tethys (WAGREICH *et al.*, 2012). Although, the position of this event is still not fully constrained, its relation to the *Radotruncana*

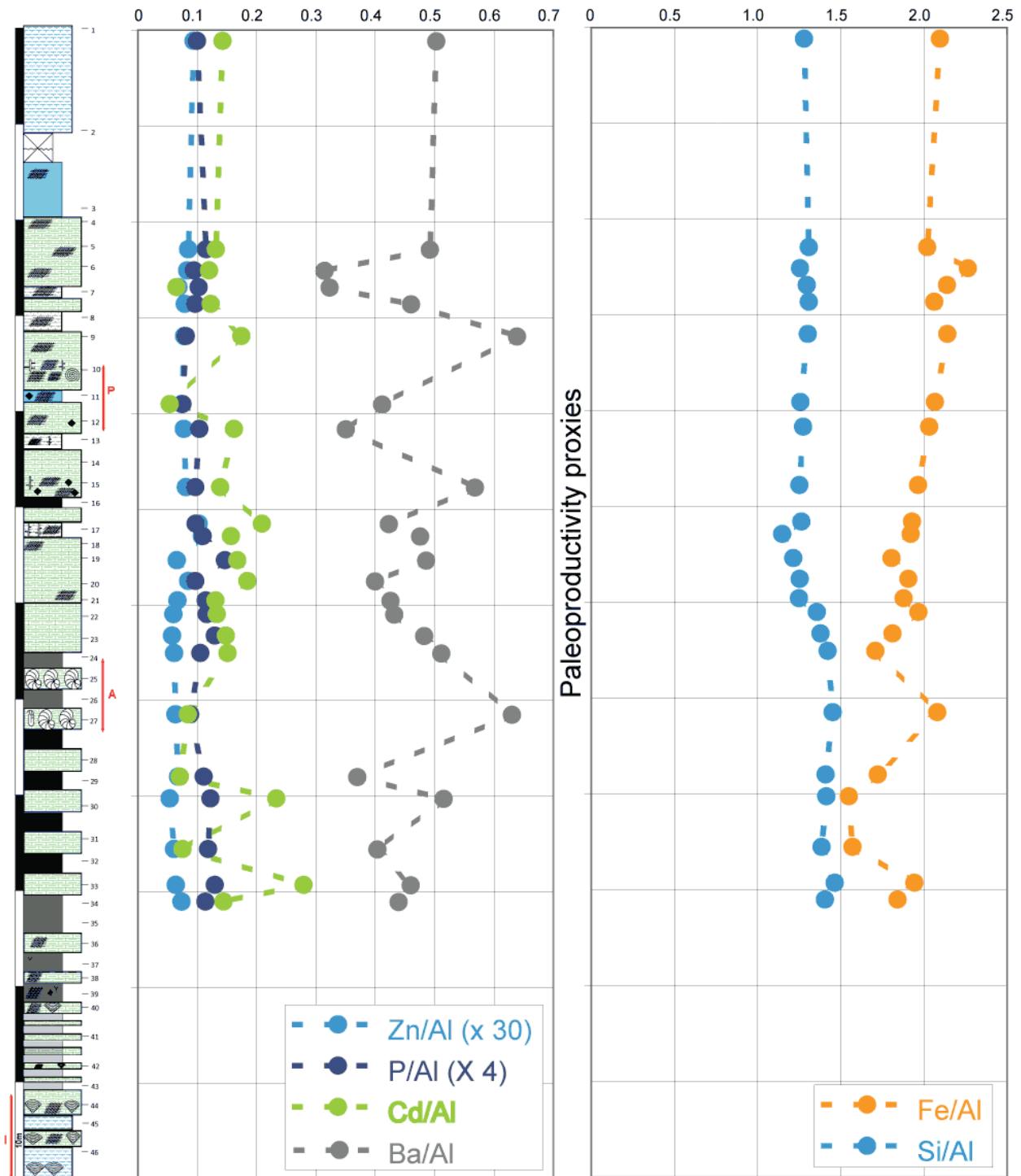


Figure 12: Ba/Al, Cd/Al, Fe/Al, P/Al, Si/Al distribution in the Bozova Formation, Mazıdađı section. Lithostratigraphic column is generalized for sample and facies comparison.

calcarata Zone and UC15cde is evident. Slight variations may be also due to regional and locally variable carbon isotope budgets but may also relate to lithostratigraphic/facies/diagenetic control/mask for the biostratigraphic appearance of the species in the stratigraphic section. The biozones in this study display the *Radotruncana calcarata* Zone and UC15cde, and the *Gansserina gansseri* Zone is not recorded here as in European sec-

tions. In addition to this, VOİGT *et al.* (2010) indicated an "inoceramid acme" in the Maastrichtian of the Pacific Ocean. This study also found a regional inoceramid acme, but in a significantly lower biostratigraphic position, and it is not a real acme zone, but a kind of locally increased relative abundance. But its position is a subject of another study.

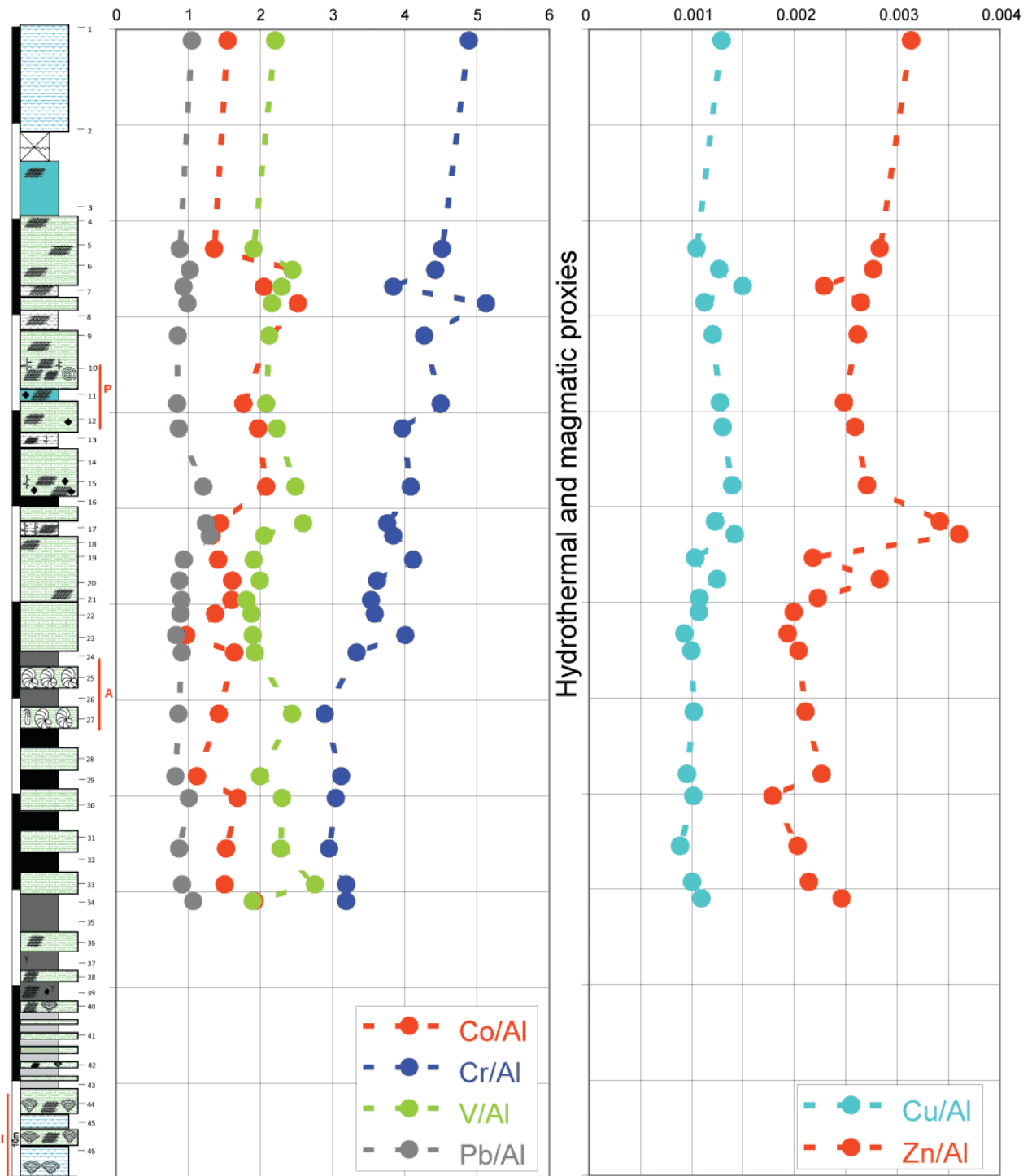


Figure 13: Co/Al, Cr/Al, V/Al, Pb/Al, Zn/Al, Cu/Al distribution in the Bozova Formation, Mazıdađı section. Lithostratigraphic column is generalized for sample and facies comparison.

8. Conclusions

The studied Upper Cretaceous pelagic succession in the Mardin-Mazıdađ area, SE Turkey on the Arabian Platform displays the lithological, chemical and paleontological characters of late Campanian oceanographic and climatic changes. The interbedded black shale, marl and clayey limestone, stable isotope changes, abundance of certain fossil groups at particular positions in the

section exhibit considerable parallel fluctuations. Biostratigraphic investigations indicate the planktonic foraminifer *Radotruncana calcarata* Zone and the calcareous nannofossil zones UC15d and CC22 at around 74-75 Ma. Stable isotopic and elemental compositions display different patterns in lower, middle and upper parts of the section. The isotope curves are divided into four different intervals in the succession.

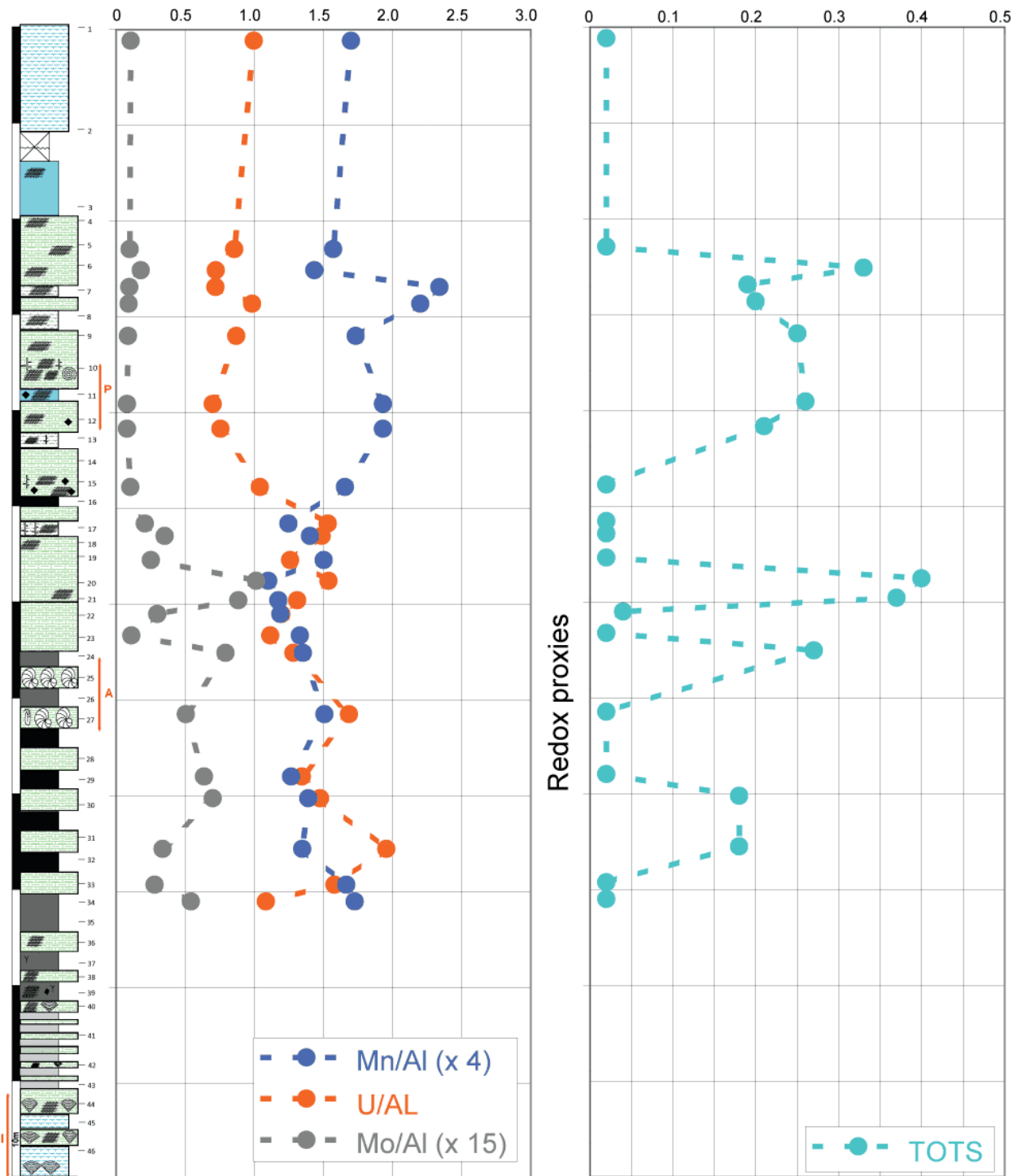


Figure 14: Mn/Al, Mo/Al, U/Al, TOTS distribution in the Bozova Formation, Mazıdađı section. Lithostratigraphic column is generalized for sample and facies comparison.

Each interval has its own characteristic features and potentially enable correlation with other successions. Carbon isotope excursions up to more than 2 per mil indicate that an oceanographic event is recorded in the carbon isotope curve in this succession. Productivity proxy elements indicate two relatively increasing trends in productivity, one in the lower part and the second in the

middle part of the studied composite section. In the upper part productivity relatively decreased in general. Redox proxy elements reveal that the lower part of the section was more dysoxic/anoxic compared to the upper part. This coincided with the occurrence of black shales in the lower part and with a negative shift in the carbon isotope curve.

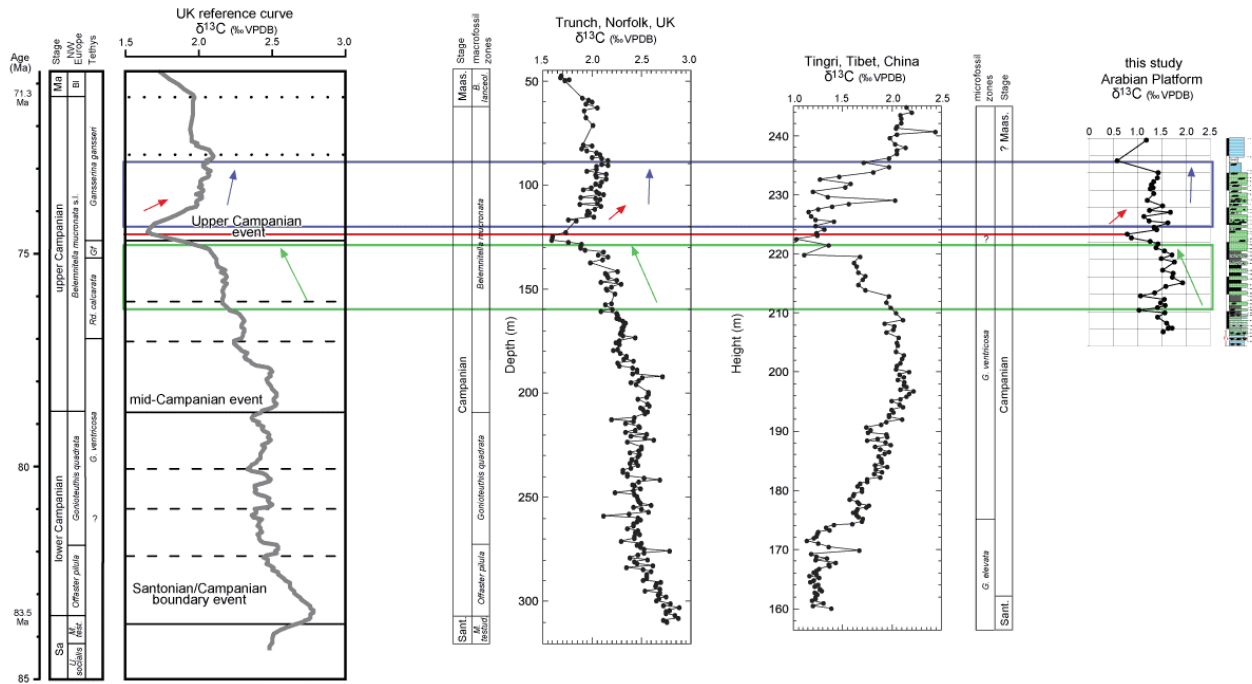


Figure 15: Comparison of the carbon stable isotope curve of the Bozova Formation, Mazıdağı section with UK (JARVIS *et al.*, 2002) and China sections (LI *et al.*, 2006). Green and yellow boxes and arrows are for comparison of rising and falling trends in different levels in isotope curves in between different regions. The red line indicates the position of the isotope excursion in the Late Campanian event.

Excess amounts of Ca/Al and Si/Al in the lower part of the section may support this interpretation of bottom waters oxygen. The Ti/Al, Zr/Al, TiO₂, and Zr curves indicate relatively more sediment influx compared to the lower part. Hydrothermal and magmatic proxy elements exhibit two relative rising trends in both upper and lower parts of the section. This suggests that sediment influx and volcanic/magmatic contribution might be mutually related. Proxy redox elements imply that the lower part of the section was more oxygen deficient compared to the upper part. This coincides with presence of common black shale occurrences in the lower part. Although there is slight a difference in biozones due to absence of index fossils, lithogenic and/or diagenetic controls, and local oceanographic variations, the carbon isotope curve patterns in the upper Campanian interval exhibit very similar patterns with the trends indicated by JARVIS *et al.* (2002, 2006) and LI *et al.* (2006), especially around the Late Campanian Event (Fig. 15). The carbon isotope excursions coincided with proxy element shifts and black shale occurrences in the same interval.

Oxygen and carbon isotope values display a more negative shift in intervals 3 and 4, following the Late Campanian Event (Figs. 10, 15). This shift can be linked to large scale paleoclimate change. The presence of fully marine, warm-water, low-latitude Tethysian oceanic conditions were revealed by nanofossils and planktonic foraminifera and a tropical humid climate condition, which were similar to present-day conditions in northeastern Australia in terms of the fossil

plants. These data support a generally warm paleoclimate in northern Arabian Platform. During the Coniacian- Maastrichtian interval the Arabian Plate was on the Boreo-tropical paleogeographic and paleoclimatic belts by presence of laterites and some coal deposits (BOUCOT *et al.*, 2013). Our record supports the presence of humid and warm conditions along the Arabian Plate in the studied area. In addition to this, SUAREZ *et al.* (2013) proposed intensive rainy conditions in the Arctic Cretaceous continental environments in relation to its hydrological cycles and polar warming. This record indirectly supports the widening of humid belts and warming effect on Cretaceous flora. Identification of types of plant fossils recognized in the study can be a clue about paleovegetation around the studied area in that time and can contribute to the understanding of the possible climatic conditions. The plant taxonomy of plant fragments as constituents of the pelagic deeper-marine formation, which are studied here for the first time in Turkey, indicate a humid hinterland and intense rainfall and flooding events to transport plant remains into the studied offshore region.

Acknowledgements

This study is dedicated to both Zeki YILMAZ, the first author's father who passed away on October 2020, and Asiye YILMAZ, his mother who passed away on December 2020. It was supported by a national scientific project (TUBITAK-111Y138, The Scientific and Technological Research Council of Turkey) and was partly financed by both UNESCO (United Nations Educational,



Scientific and Cultural Organization) IGCP-609 (The Council of the International Geoscience Program) and the Austrian Academy of Sciences, International Programs. Authors are also thankful to the Department of Paleontology, National Museum Prague, Czech Republic, the Department of Geodynamics and Sedimentology, University of Vienna, Austria and the Department of Geological Engineering, Middle East Technical University, Ankara, Turkey. One coauthor (J.K.) was financially supported by the Ministry of Culture of the Czech Republic (IP DKRVO, 2019/2.II.a, National Museum, 00023272). Last but not least, the authors thank the anonymous referees and *Carnets'* editors for their comments and suggestions that significantly helped improving the original manuscript.

Bibliographic references

- ACIKALIN S., VELLEKOOP J., YILMAZ I.O., SMIT J., GORDERIS S., VONHOF H., SPEIJER R., WOELDERS, L., OCAKOĞLU F., ALTINER S. O., FORNACIARI E. & BRINKHUIS H. (2015).- Geochemical and paleontological characterization of a new K-Pg Boundary locality from the northern branch of the Neotethys; Mudurnu - Göynük Basin, NW Turkey.- *Cretaceous Research*, vol. 52, p. 251-267.
- ALA M.A. & MOSS B.J. (1979).- Comparative petroleum geology of southeast Turkey and northeast Syria.- *Journal of Petroleum Geology*, vol. 1, no. 4, p. 3-27.
- ANDRUCHOW-COLOMBO, A., ESCAPA, I.H., CÚNEO R.N. & GANDOLFO, M.A. (2018).- *Araucaria lefipansensis* (Araucariaceae), a new species with dimorphic leaves from the Late Cretaceous of Patagonia, Argentina.- *American Journal of Botany*, Brooklyn - NY, vol. 105, no. 6, p. 1067-1087.
- BARALE G. (1981).- La paléoflore jurassique du Jura Français : Étude systématique, aspects stratigraphiques et paléoécologiques.- *Documents des Laboratoires de Géologie*, Lyon, vol. 81, 467 p.
- BAYER E. (1893).- O rostlinstvu vrstev březenských [On Flora of the Březno Member].- *Věstník královské české společnosti nauk (Třída matematicko-přírodovědecká) [Sitzungsberichte der Königl. böhmischen Gesellschaft der Wissenschaften (Mathematisch naturwissenschaftliche Classe)]*, Prague, vol. 39, p. 1-50.
- BECKMANN B., WAGNER T. & HOFMANN P. (2005).- Linking Coniacian-Santonian (OAE3) black-shale deposition to African climate variability: A reference section from the eastern tropical Atlantic at orbital time scales (ODP site 959, off Ivory Coast and Ghana). In: HARRIS N.B. (ed.), The deposition of organic-carbon-rich sediments: Models, mechanisms, and consequences.- *SEPM, Special Publication*, vol. 82, p. 125-143.
- BEER H. (1966).- Mardin-Derik-Mazıdağı çevresindeki fosfatlı tabakaların jeolojisi.- *Bulletin of Mineral Research and Exploration Institute*, Ankara, Turkey, vol. 66, p. 104-120.
- BISHOP J.W., OSLEGER D.A., MONTANEZ I.P. & SUMMER D.Y. (2014).- Meteoric diagenesis and fluid-rock interaction in the Middle Permian Capitan backreef: Yates Formation, Slaughter Canyon, New Mexico.- *American Association of Petroleum Geologists Bulletin*, Ankara, Turkey, vol. 98, no. 8, p. 1495-1519.
- BOLL H.M., SAUNDERS K. & NIELSEN P. (1985).- Plankton stratigraphy.- Cambridge University Press, 599 p.
- BOUCOT A.J., CHEN XU C., SCOTSESE C.R. & MORLEY R.J. (2013).- Phanerozoic paleoclimate: An atlas of lithologic indicators of climate.- *SEPM Concepts in Sedimentology and Paleontology*, Tulsa - OK, vol. 11, 478 p.
- BURDIGE D.J. (2006).- Geochemistry of marine sediments.- Princeton University Press, Princeton - NJ, 609 p.
- BURNETT J.A. (1998).- Upper Cretaceous. In: BROWN P.R. (ed.), Calcareous nannofossil biostratigraphy.- Chapman & Hall, Cambridge, p. 132-199.
- CATER J.M.L. & GILLCRIST J.R. (1994).- Karstic reservoirs of the Mid-Cretaceous Mardin Group, SE Turkey: Tectonic and eustatic controls on their genesis, distribution and preservation.- *Journal of Petroleum Geology*, vol. 17, no. 3, p. 253-278.
- CHENOT E., PELLENARD P., MARTINEZ, M., DECONINCK J-F., AMIOTTE-SUCHET P., THIBAUT N., BRUNEAU L., COCQUEREZ T., LAFFONT R., PUCÉAT E. & ROBASZYNSKI F. (2016).- Clay mineralogical and geochemical expressions of the "Late Campanian Event" in the Aquitaine and Paris basins (France): Palaeoenvironmental implications.- *Palaeogeography, Palaeoclimatology, Palaeoecology*, vol. 447, p. 42-52.
- CHRISTENSEN E.R. (1982).- A model for radionuclides in sediments influenced by mixing and compaction.- *Journal of Geophysical Research*, vol. 87, no. C1, p. 566-572.
- COLE D.B., ZHANG S. & PLANAVSKY N.J. (2017).- A new estimate of detrital redox-sensitive metal concentrations and variability in fluxes to marine sediments.- *Geochimica et Cosmochimica Acta*, vol. 215, p. 337-353.
- ÇORUH T., YAKAR H. & EDIGER V.S. (1997).- Biostratigraphic atlas of the autochthonous succession of southeastern Anatolia.- *Turkish Petroleum Corporation, Special Publication*, Ankara, Turkey, vol. 30, 510 p. (in Turkish).
- DEMINA L.L. & GALKIN S.V. (2016).- Trace metal biogeochemistry and ecology of deep-sea hydrothermal vent systems.- *The Handbook of Environmental Chemistry*, vol. 50, 207 p.
- DOLUDENKO M.P. & ORLOVSKAIA E.R. (1976).- Jurassic flora of Karatau [Iurskaia flora Karatau].- Nauka, Moscow, 260 p.



- KURU F. (1987).- Biostratigraphy of the Bozova Formation Derik-Mazıdağ, Mardin, SE Turkey.- 7th Biannual Petroleum Congress of Turkey, Ankara, Turkey, p. 154-164.
- EDELMAN-FURSTENBERG Y. (2009).- Cyclic upwelling facies along the Late Cretaceous southern Tethys (Israel): Taphonomic and ichnofacies evidence of a high-productivity mosaic.- *Cretaceous Research*, vol. 30, p. 847-863.
- ERKMEN U. & SADEK A. (1981).- Contribution to the stratigraphy of the Germav Formation (Late Cretaceous-Early Tertiary) in SE Turkey by means of dinoflagellates and nannoplankton.- *Neues Jahrbuch für Geologie und Paläontologie Monatshefte*, Stuttgart, vol. 3, p. 129-141.
- FARJON A. (2010).- A handbook of the world's conifers.- Brill Academic Publishers, Leiden, 1150 p.
- FLÜGEL E. (2004).- Microfacies of carbonate rocks: Analysis, interpretation and application.- Springer-Verlag, New York - NY, 976 p.
- FONTAINE J.M., MONOD O., BRAUD J. & PERINCEK D. (1989).- The Hezan Units: a fragment of the south neo Tethyan passive continental margin in SE Turkey.- *Journal of Petroleum Geology*, vol. 12, p. 29-50.
- GOSWAMI V., SINGH S.K., BHUSHAN R. & RAI V.K. (2012).- Temporal variations in ⁸⁷Sr/⁸⁶Sr and eNd in sediments of the southeastern Arabian Sea: Impact of monsoon and surface water circulation.- *Geochemistry Geophysics Geosystems*, vol. 13, p. 1-13.
- GRADSTEIN F.M., OGG J. & HILGEN F. (2012).- The Geological Time Scale, 2012, 1st Edition.- Elsevier, Amsterdam, 1144 p.
- HAQ B.U. (2014).- Cretaceous eustasy revisited.- *Global and Planetary Change*, vol. 113, p. 44-58.
- HAQ B.U. & AL-QAHTANI M. (2005).- Phanerozoic cycles of sea-level change on the Arabian Platform.- *GeoArabia*, Manama, vol. 10, no. 2, p. 127-160.
- HARRIS T.M. (1979).- The Yorkshire Jurassic flora, V.- Trustees of the British Museum (Natural History), London, 166 p.
- HAY W.W. & FLOEGEL S. (2012).- New thoughts about the Cretaceous climate and oceans.- *Earth-Science Reviews*, vol. 115, p. 262-272.
- HOEFS J. (2009).- Stable isotope geochemistry. Sixth edition.- Springer-Verlag, Berlin Heidelberg, 285 p.
- HORSTINK F. (1970).- The Late Cretaceous and Tertiary geological evolution of eastern Turkey.- *Proceedings of the First Petroleum Congress of Turkey*, p. 25-41.
- HOŞGÖR I. & KOSTÁK M. (2012).- Occurrence of the Late Cretaceous belemnite *Belemnitella* in the Arabian Plate (Hakkari, SE Turkey) and its palaeogeographic significance.- *Cretaceous Research*, vol. 37, p. 35-42.
- HOŞGÖR I. & YILMAZ I.O. (2019).- Paleogeographic northeastern limits of *Aphrodina dutruegi* (COCQUAND, 1862) (Heterodonta, Bivalvia) from the Cenomanian of the Arabian Platform.- *Rivista Italiana di Paleontologia e Stratigrafia*, Milano, Italy, vol. 125, no. 2, p. 421-431.
- HU X., WAGREICH M. & YILMAZ I.O. (2012).- Marine rapid environmental/climatic change in the Cretaceous greenhouse world.- *Cretaceous Research*, vol. 38, p. 1-6.
- HUTH J. (2002).- Introducing the Bunya Pine, a noble denizen of the scrub.- *Queensland Review*, Cambridge (UK), vol. 9, no. 2, p. 7-20.
- İŞBİLİR M., KIRICI S. & YILMAZ Z. (1992).- Evaluation of the Upper Cretaceous carbonate reservoirs in the platform region of Petroleum district X, SE Anatolia.- 9th Petroleum Congress of Turkey, Abstract Book.- In: Turkish Association of Petroleum Geologists Publication, Ankara, p. 436-442.
- JARVIS I., MABROUK A., MOODY R.T.J. & CABERA S. (2002).- Late Cretaceous (Campanian) carbon isotope events, sea-level change and correlation of the Tethyan and Boreal realms.- *Palaeogeography, Palaeoclimatology, Palaeoecology*, vol. 188, p. 215-248.
- JARVIS I., GALE A.S., JENKYN H.C. & PEARCE M.A. (2006).- Secular variation in Late Cretaceous carbon isotopes: A new $\delta^{13}\text{C}$ carbonate reference curve for the Cenomanian-Campanian (99.6-70.6 Ma).- *Geological Magazine*, vol. 143, no. 5, p. 561-608.
- JUNG W. (1996).- Die Araucarien - Wanderer zwischen Nord und Süd. In: DERNBACH U. (ed.), *Versteinerte Wälder*.- D'Oro, Heppenheim, p. 170-181.
- KELLOG H.E. (1960).- The Geology of the Derik-Mardin area.- Report of the Exploration Division, American Overseas Petroleum Ltd, Ankara, 27 p.
- KERSHAW P. & WAGSTAFF B. (2001).- The southern conifer family Araucariaceae: history, status, and value for paleoenvironmental reconstruction.- *Annual Review of Ecology and Systematics*, New York, vol. 32, p. 397-414.
- KÖYLÜOĞLU M. (1988).- The paleontology and stratigraphy of the Beloka Formation in which Kasrik and Semikan phosphate deposits are found, Mardin-Mazıdağı, Southeast Turkey.- *Bulletin of the Turkish Association of Petroleum Geologists*, Ankara, Turkey, vol. 1-2, p. 141-151.
- KRASSILOV V.A. (1978).- Araucariaceae as indicators of climate and palaeolatitudes.- *Review of Palaeobotany and Palynology*, vol. 26, p. 113-124.
- KUNZMANN L. (2007a).- Araucariaceae (Pinopsida): Aspects in palaeobiogeography and palaeobiodiversity in the Mesozoic.- *Zoologischer Anzeiger*, vol. 246, p. 257-277.
- KUNZMANN L. (2007b).- Neue Untersuchungen zu *Araucaria* JUSSIEU aus der europäischen Kreide.- *Palaeontographica*, Abt. B, Stuttgart, vol. 276, no. 4-6, p. 97-131.



- KVAČEK J., BARRÓN E., HEŘMANOVÁ Z., MENDES M.M., KARCH J., ŽEMLIČKA J. & DUDÁK J. (2018).- Araucarian conifer from late Albian amber of northern Spain.- *Special Papers in Palaeontology*, vol. 4, no. 4, p. 643-656.
- KVAČEK J., YILMAZ I., HOŞGÖR I. & MENDES M.M. (2019).- New araucarian conifer from the Late Cretaceous (Campanian-Maastrichtian) of southeastern Turkey.- *International Journal of Plant Sciences*, vol. 180, no. 6, p. 597-606.
- LEES J.A. (2002).- Calcareous nannofossils biogeography illustrates palaeoclimate change in the Late Cretaceous Indian Ocean.- *Cretaceous Research*, vol. 23, p. 537-634.
- LI X., JENKYN H.C., WANG C., HU X., CHEN X., WEI Y., HUANG Y. & CUI J. (2006).- Upper Cretaceous carbon- and oxygen- isotope stratigraphy of hemipelagic carbonate facies from southern Tibet, China.- *Journal of the Geological Society*, London, vol. 163, p. 375-382.
- LIGUORI B.T.P., ALMEIDA M.G. de & REZENDE C.E. (2016).- Barium and its importance as an indicator of (paleo)productivity.- *Anais da Academia Brasileira de Ciências (Annals of the Brazilian Academy of Sciences)*, Rio de Janeiro, vol. 88, no. 4, p. 2093-2103.
- LOCKLAIR R., SAGEMAN B. & LERMAN A. (2011).- Marine carbon burial flux and the carbon isotope record of Late Cretaceous (Coniacian-Santonian) Oceanic Anoxic Event III.- *Sedimentary Geology*, vol. 235, no. 1-2, p. 38-49.
- MCKAY J.L., PEDERSEN T.F. & MUCCI A. (2007).- Sedimentary redox conditions in continental margin sediments (N.E. Pacific): Influence on the accumulation of redox-sensitive trace metals.- *Chemical Geology*, vol. 238, p. 180-196.
- MULAYIM O., MANCINI E., CEMEN I. & YILMAZ I.O. (2016).- Upper Cenomanian-Lower Campanian Derdere and Karababa formations in the Çemberlitaş oil field, southeastern Turkey: Their microfacies analyses, depositional environments, and sequence stratigraphy.- *Turkish Journal of Earth Sciences*, Ankara, vol. 25, p. 46-63.
- OHSAWA T., NISHIDA H. & NISHIDA M. (1995).- *Yezonia*, a new section of *Araucaria* (Araucariaceae) based on permineralized vegetative and reproductive organs of *A. vulgaris* comb. nov. from the Upper Cretaceous of Hokkaido, Japan.- *Journal of Plant Research*, vol. 108, p. 25-39.
- ÖZER S. (1993).- Rudist carbonate ramp in southeastern Anatolia, Turkey.- *American Association of Petroleum Geologists, Special Publication*, vol. 56, p. 163-171.
- OWEN R.M. & OLIVAREZ A.M. (1988).- Geochemistry of rare earth elements in Pacific hydrothermal sediments.- *Marine Chemistry*, vol. 25, p. 183-196.
- PANTI C., PUJANA R.R., ZAMAOLA, M.C. & ROMERO E.J. (2012).- Araucariaceae macrofossil record from South America and Antarctica.- *Alcheringa*, vol. 36, no. 1, p. 1-22.
- PAYTAN A. (2009).- Ocean paleoproductivity. In: GORNITZ V. (ed.), *Encyclopedia of paleoclimatology and ancient environments.- Encyclopedia of Earth Sciences Series*, p. 643-651.
- PERCH-NIELSEN K. (1985).- Mesozoic calcareous nannofossils. In: BOLLI H.M., SAUNDERS J.B. & PERCH-NIELSEN K. (eds.), *Plankton stratigraphy.- Cambridge University Press*, p. 329-426.
- PERDIOU A., THIBAUT N., ANDERSKOUV K., BUCHEM F. van, BUIJS G.J.A. & BJERRUM C.J. (2015).- Orbital calibration of the late Campanian carbon isotope event in the North Sea.- *Journal of the Geological Society*, vol. 173, no. 3, p. 504-507.
- POINAR G.O. Jr & MILKI R. (2001).- Lebanese amber. The oldest insect ecosystem in fossilized resin.- Oregon State University Press, Corvallis - OR, 96 p.
- POINAR G.O. Jr, LAMBERT J.B. & WU Y. (2007).- Araucarian source of fossiliferous Burmese amber: Spectroscopic and anatomical evidence.- *Journal of the Botanical Research Institute of Texas*, Fort Worth - TX, vol. 1, p. 449-455.
- PUFAHL P.K., GRIMM K.A., ABED A.M. & SADAGAH R.M.Y. (2003).- Upper Cretaceous (Campanian) phosphorites in Jordan: Implications for the formation of a south Tethyan phosphorite giant.- *Sedimentary Geology*, vol. 161, p. 175-205.
- SUAREZ C.A., LUDVIGSON G.A., GONZALEZ L.A., FIORILLO A.R., FLAIG P.P. & MCCARTHY P.J. (2013).- Use of multiple oxygen isotope proxies for elucidating Arctic Cretaceous palaeo-hydrology. In: BOJAR, A.V., MELINTE-DOBRIANESCU M.C. & SMIT J. (eds.), *Isotopic studies in Cretaceous research.- Geological Society, Special Publications*, London, vol. 382, p. 185-202.
- STOCKEY R.A. (1980a).- Anatomy and morphology of *Araucaria sphaerocarpa* CARRUTHERS from the Jurassic Inferior Oolite of Bruton, Somerset.- *Botanical Gazette*, vol. 141, p. 116-124.
- STOCKEY R.A. (1980b).- Jurassic araucarian cone from southern England.- *Palaeontology*, vol. 23, p. 657-666.
- STOCKEY R.A. (1982).- The Araucariaceae: An evolutionary perspective.- *Review of Palaeobotany and Palynology*, vol. 37, p. 133-154.
- STOCKEY R.A., NISHIDA H. & NISHIDA M. (1992).- Upper Cretaceous araucarian cones from Hokkaido: *Araucaria nihongii* sp. nov.- *Review of Palaeobotany and Palynology*, vol. 72, p. 27-40.
- STOCKEY R.A., NISHIDA H. & NISHIDA M. (1994).- Upper Cretaceous araucarian cones from Hokkaido and Saghalien: *Araucaria nipponensis* sp. nov.- *International Journal of Plant Sciences*, vol. 155, p. 806-815.
- STOCKEY R.A. & TAYLOR T.N. (1978).- Cuticular features and epidermal patterns in the genus *Araucaria* de JUSSIEU.- *Botanical Gazette*, vol. 139, p. 490-498.



- SUNGURLU O. (1974).- Geology of the northern part of Petroleum District-6.- Second Petroleum Congress of Turkey, p. 85-107.
- THIBAUT N. & GARDIN S. (2006).- Maastrichtian calcareous nannofossil biostratigraphy and paleoecology in the Equatorial Atlantic (Demerara Rise, ODP Leg, 207 Hole 1258A).- *Revue de Micropaleontologie*, vol. 49, no. 4, p., 199-214.
- THIBAUT N. & GARDIN S. (2010).- The calcareous nannofossil response to the end-Cretaceous warm event in the Tropical Pacific.- *Palaeogeography, Palaeoclimatology, Palaeoecology*, vol. 291, p. 239-252.
- THIBAUT N., HARLOU R., SCHOVSBO N.H., STEMMERIK L. & SURLYK F. (2015).- Late Cretaceous (Late Campanian-Maastrichtian) sea surface temperature record of the Boreal Chalk Sea.- *Climate of the Past Discussions*, vol. 11, p. 5049-5071.
- TRIBOVILLARD N., ALGEO T.J., LYONS T. & RIBOULLEAU A. (2006).- Trace metals as paleoredox and paleoproductivity proxies: An update.- *Chemical Geology*, vol. 232, p. 12-32.
- UMUT M. (2011).- MTA-Diyarbakır-N 44 Paftası, no. 168.- 1/100 000 ölçekli Türkiye Jeoloji Haritası, 42 p.
- VOIGT S., FRIEDRICH O., NORRIS R.D. & SCHÖNFELD J. (2010).- Campanian - Maastrichtian carbon isotope stratigraphy: Shelf-ocean correlation between the European shelf sea and the tropical Pacific Ocean.- *Newsletters on Stratigraphy*, vol. 44, no. 1, p. 57-72.
- VOIGT S., GALE A.S., JUNG C. & JENKYN H.C. (2012).- Global correlation of Upper Campanian- Maastrichtian successions using carbon isotope stratigraphy: Development of a new Maastrichtian timescale.- *Newsletters on Stratigraphy*, vol. 45, no. 1, p. 25-53.
- WAGREICH M. (2009).- Coniacian-Santonian oceanic red beds and their link to Oceanic Anoxic Event 3. Cretaceous oceanic red beds: Stratigraphy, composition, origins, and paleoceanographic and paleoclimatic significance.- *SEPM (Society for Sedimentary Geology) Special Publication*, vol. 91, p. 235-242.
- WAGREICH M., HOHENEGGER J. & NEUHUBER S. (2012).- Nannofossil biostratigraphy, strontium and carbon isotope stratigraphy, cyclostratigraphy and an astronomically calibrated duration of the late Campanian *Radotruncana calcarata* Zone.- *Cretaceous Research*, vol. 38, p. 80-96.
- WANG Y., ZHANG W., ZHENG S., JINTASAKUL P., GROTE P.J. & BOOCHAI N. (2006).- Recent advances in the study of Mesozoic-Cenozoic petrified wood from Thailand.- *Progress in Natural Science*, vol. 16, p. 501-506.
- WENDLER I. (2013).- A critical evaluation of carbon isotope stratigraphy and biostratigraphic implications for Late Cretaceous global correlation.- *Earth-Science Reviews*, vol. 126, p. 116-146.
- YILMAZ I.O., COOK T.D., HOŞGÖR I., WAGREICH M., REBMAN K. & MURRAY A. (2018).- The upper Coniacian to upper Santonian drowned Arabian carbonate platform, the Mardin-Mazidag area, SE Turkey: Sedimentological, stratigraphic, and ichthyofaunal records.- *Cretaceous Research*, vol. 84, p. 153-167.
- ZAREI E. & GHASEMI-NEJAD E. (2015).- Sequence stratigraphy of the Gurpi Formation (Campanian-Paleocene) in southwest of Zagros, Iran, based on palynomorphs and foraminifera.- *Arabian Journal of Geosciences*, vol. 8, p. 4011-4023.



Appendices

Appendix 1

Sample	Meters (from top)	$\delta^{13}\text{C}$	$\delta^{18}\text{O}$
1	0.00	1.17734	-3.85454
2	2.50	0.57259	-4.03190
3	5.00	1.42260	-3.73683
4	6.50	1.40722	-3.83000
5	8.00	1.33093	-3.69973
6	10.50	1.28293	-3.81409
7	12.50	1.31809	-3.84412
8	14.50	1.25887	-3.84600
9	16.50	1.33220	-3.79000
10	18.50	1.19688	-3.98420
11	21.00	1.51338	-3.79411
12	23.50	1.24377	-3.82621
13	25.50	1.67649	-4.01545
14	27.50	1.12682	-4.23000
15	30.00	1.23399	-4.23033
16	32.25	1.62347	-3.85682
17	34.25	1.33835	-4.05860
18	36.75	1.39300	-4.02753
19	38.75	0.78135	-3.77318
20	40.75	0.86824	-3.81722
21	42.75	1.25688	-3.84761
22	43.95	1.42000	-3.61000
23	47.65	1.37994	-3.90945
24	49.45	1.55298	-3.67717
25	51.45	1.70782	-3.48377
26	54.45	1.48503	-3.79877
27	55.45	1.76000	-3.60000
28	58.95	1.51548	-3.62155
29	63.45	1.73337	-3.63501
30	73.25	1.71624	-3.70885
31	75.25	1.92921	-3.45896
32	76.75	1.58000	-3.82000
33	77.25	1.35022	-3.55542
34	78.75	1.05768	-4.17431
35	80.75	1.55000	-3.73000
36	82.75	1.47429	-3.78056
37	86.25	1.56610	-3.65129
38	87.75	1.41078	-3.53936
39	89.75	1.02593	-4.21973
40	91.25	1.56073	-3.74889
41	91.75	1.41000	-3.48000
42	92.75	1.60000	-3.84000
43	95.75	1.71200	-3.57824
44	98.75	1.63076	-3.96437
45	100.75	1.52704	-3.60657



Appendix 2

	SiO ₂	Al ₂ O ₃	Fe ₂ O ₃	CaO	P ₂ O ₅	TiO ₂	MnO	Cr ₂ O ₃	TOTS	Sr	Mo	Zn	Cu	Pb	Cd	Ba	Co	V	Ni	Zr
sample	%	%	%	%	%	%	%	%	%	PPM	PPM	PPM	PPM	PPM	PPM	PPM	PPM	PPM	PPM	PPM
1	13.00	2.65	1.86	42.22	0.08	0.23	0.04	0.014	0.02	1130	0.1	44	18.1	3.3	0.2	50	6.3	45	70	29.2
4	14.40	2.87	1.94	40.54	0.10	0.27	0.04	0.014	0.02	1044	0.1	43	15.9	3.0	0.2	53	6.0	42	84	33.5
5	15.11	3.14	2.38	39.48	0.09	0.30	0.04	0.015	0.33	1055	0.2	46	21.1	3.8	0.2	37	11.8	59	84	34.0
6	14.36	2.89	2.07	40.20	0.09	0.27	0.06	0.012	0.19	1138	0.1	35	22.9	3.2	0.1	35	9.1	51	77	32.3
7	15.39	3.07	2.12	39.19	0.09	0.29	0.06	0.017	0.20	1060	0.1	43	18.3	3.6	0.2	53	11.9	51	87	35.1
9	16.22	3.25	2.33	37.89	0.08	0.28	0.05	0.015	0.25	1056	0.1	45	20.7	3.3	0.3	78	10.6	53	85	34.6
11	16.89	3.50	2.42	37.01	0.08	0.33	0.06	0.017	0.26	1063	0.1	46	23.6	3.5	0.1	54	9.5	56	77	36.6
12	17.10	3.50	2.38	36.94	0.11	0.30	0.06	0.015	0.21	983.7	0.1	48	24.1	3.6	0.3	46	10.6	60	80	36.0
15	13.05	2.72	1.79	41.81	0.08	0.21	0.04	0.012	0.02	1117	0.1	39	20.1	3.9	0.2	58	8.7	52	58	27.4
17	13.13	2.71	1.75	41.50	0.08	0.21	0.03	0.011	0.02	1223	0.2	49	17.6	4.0	0.3	43	6.0	54	60	28.7
18	10.62	2.41	1.55	44.03	0.08	0.18	0.03	0.010	0.02	1215	0.3	46	18.1	3.7	0.2	43	4.9	38	53	23.5
19	10.48	2.25	1.36	44.43	0.10	0.20	0.03	0.010	0.02	1170	0.2	26	12.3	2.5	0.2	41	4.9	33	38	22.7
20	14.76	3.07	1.96	40.86	0.09	0.27	0.03	0.012	0.40	1137	1.1	46	20.3	3.2	0.3	46	7.6	47	56	32.7
21	13.81	2.88	1.81	41.84	0.10	0.25	0.03	0.011	0.37	1170	0.9	34	16.4	3.1	0.2	46	7.1	40	52	29.2
22	14.77	2.84	1.87	40.48	0.10	0.25	0.03	0.011	0.04	1229	0.3	30	16.1	3.0	0.2	46	6.0	41	46	30.4
23	13.44	2.54	1.54	42.52	0.10	0.21	0.03	0.011	0.02	1213	0.1	26	12.5	2.5	0.2	46	3.8	37	37	25.8
24	13.63	2.50	1.43	43.06	0.08	0.21	0.03	0.009	0.27	1243	0.7	27	13.2	2.7	0.2	48	6.3	37	52	24.6
27	12.47	2.24	1.56	43.64	0.06	0.17	0.03	0.007	0.02	1367	0.4	25	12.1	2.3	0.1	53	4.9	42	35	23.3
29	14.43	2.67	1.54	41.77	0.09	0.21	0.03	0.009	0.02	1331	0.6	32	13.5	2.6	0.1	37	4.6	41	45	26.6
30	13.18	2.43	1.26	43.37	0.09	0.20	0.03	0.008	0.18	1345	0.6	23	13.1	2.9	0.3	47	6.3	43	33	30.2
32	13.34	2.51	1.32	42.93	0.09	0.19	0.03	0.008	0.18	1405	0.3	27	11.8	2.6	0.1	38	5.9	44	44	25.6
33	11.40	2.03	1.32	44.71	0.08	0.16	0.03	0.007	0.02	1359	0.2	23	10.8	2.2	0.3	35	4.7	43	31	21.7
34	14.07	2.61	1.61	41.74	0.09	0.22	0.04	0.009	0.02	1155	0.5	34	15.1	3.3	0.2	43	7.7	38	54	26.4